Cellular and subcellular interactions of graphene-based materials with cancerous and non-cancerous cells

Advanced Drug Delivery Reviews 189 (2022) 114467

Contents lists available at ScienceDirect

Advanced Drug Delivery Reviews

journal homepage: www.elsevier.com/locate/adr

Cellular and subcellular interactions of graphene-based materials with cancerous and non-cancerous cells

Shadi Rahimi [a,*], Yanyan Chen [a], Mohsen Zareian [a,b], Santosh Pandit [a], Ivan Mijakovic [a,c,*]

[a] Department of Biology and Biological Engineering, Chalmers University of Technology, Göteborg 41296, Sweden
[b] State Key Laboratory of Bio-based Material and Green Paper-making, Qilu University of Technology, Jinan, China
[c] The Novo Nordisk Foundation Center for Biosustainability, Technical University of Denmark, 2800 Kgs. Lyngby, Denmark

ARTICLE INFO

Article history:
Received 25 February 2022
Revised 22 July 2022
Accepted 26 July 2022
Available online 29 July 2022

Keywords:
Cancer
Drug delivery
Graphene oxide
Graphene-based materials
Metastasis treatment
Size
Surface chemistry

ABSTRACT

Despite significant advances in early detection and personalized treatment, cancer is still among the leading causes of death globally. One of the possible anticancer approaches that is presently receiving a lot of attention is the development of nanocarriers capable of specific and efficient delivery of anticancer drugs. Graphene-based materials are promising nanocarriers in this respect, due to their high drug loading capacity and biocompatibility. In this review, we present an overview on the interactions of graphene-based materials with normal mammalian cells at the molecular level as well as cellular and subcellular levels, including plasma membrane, cytoskeleton, and membrane-bound organelles such as lysosomes, mitochondria, nucleus, endoplasmic reticulum, and peroxisome. In parallel, we assemble the knowledge about the interactions of graphene-based materials with cancerous cells, that are considered as the potential applications of these materials for cancer therapy including metastasis treatment, targeted drug delivery, and differentiation to non-cancer stem cells. We highlight the influence of key parameters, such as the size and surface chemistry of graphene-based materials that govern the efficiency of internalization and biocompatibility of these particles *in vitro* and *in vivo*. Finally, this review aims to correlate the key parameters of graphene-based nanomaterials specially graphene oxide, such as size and surface modifications, to their interactions with the cancerous and non-cancerous cells for designing and engineering them for bio-applications and especially for therapeutic purposes.

Contents

* Corresponding authors at: Department of Biology and Biological Engineering, Chalmers University of Technology, Kemivägen 10, Göteborg 41296, Sweden.
E-mail addresses: shadir@chalmers.se (S. Rahimi), ivan.mijakovic@chalmers.se (I. Mijakovic).

https://doi.org/10.1016/j.addr.2022.114467
0169-409X/

1. Introduction

According to the World Health Organization, the second most common global cause of death is cancer, causing around one in six deaths and an estimated total of 9.6 million deaths in 2018 [1]. Among many strategies currently being developed to tackle effective diagnostics and treatment of cancer, nanotechnology offers an interesting venue of developing specific nanocarriers for precise topical delivery of anticancer drugs.

Graphene a single layer, hexagonally packed 2D carbon sheet consisting of sp2-hybridized carbon atoms is an attractive candidate for diverse applications [2]. It has a high surface area, large delocalized electron system, outstanding photothermal, mechanical and electrical properties. However, the hydrophobic nature of pristine graphene hinders its biomedical and biological application. Thus, introducing oxidative groups on graphene sheets through oxidation processes generates various graphene derivatives (graphene-based materials) including graphene oxide (GO), reduced GO (rGO), hydrated GO (hGO), and graphene quantum dots (GQDs), that feature good hydrophilicity and thereby of great interest for potential applications specially in the biomedical field [3]. Wick et al., (2014) considered three fundamental properties for graphene derivatives including lateral size, number of layers, and carbon-to-oxygen (C/O) ratio that affect the biosafety profile of these materials [4]. They classified GO and rGO as normally single layer materials with C/O ratio of 4:1 to 2:1 for GO and 12:1 up to 246:1 for rGO.

In the biomedical field, graphene and its derivatives have been used as a drug cargo system to deliver therapeutic agents to cancer cells [5]. The oxygenated derivative of graphene, graphene oxide (GO), has particularly interesting features for drug delivery. It contains alcohol, carboxyl and epoxide functional groups, which result in higher water dispersibility and can be used as chemical handles for covalent modifications. Moreover, it has been argued that the water layer associated to oxidation sites hydrophilic functional groups on the GO surface enhances biocompatibility of this material, and even to stimulated growth and proliferation of mammalian cells in contact with GO [6,7]. Other properties of GO that have been exploited for various anticancer applications include the strong near-infrared absorbance of GO that has been used for cancer-targeting photothermal therapy and imaging [8], and drug loading, targeting and delivery capacity which has been used for on-site delivery and release of antitumor drugs [9]. Finally, GO nanoflakes in the size range of 100–200 nm were found to inhibit tumor growth and cancer cell metastasis [10,11].

The existing review articles on drug delivery using graphene-based nanomaterials focus largely on their physicochemical properties and optimal approaches for fabrication of effective and safe nanocarriers [12,13]. In this review, we aim to correlate the key parameters of graphene-based nanomaterials specially GO, such as size and surface modifications, to their interactions with the cancerous and non-cancerous cells in cell culture and *in vivo*. This review aims to assist the researchers in considering the chemical and physical properties of graphene-based materials when they design and engineer them for bio-applications and especially for therapeutic purposes.

2. Functionalization and biocompatibility

Biocompatibility and biosafety are the major concerns when exploring biomedical applications of graphene nanomaterials. Pristine graphene nanomaterials exhibit size-, dose- and time-dependent toxicity to various cell lines due to direct interaction with cell membrane or crucial components inside cells [14,15]. To address these issues, functionalization of graphene nanomaterials with biocompatible molecules to manipulate their physicochemical properties is a promising method [3,12,16], leading to lower cytotoxicity and better biocompatibility both in *in vitro* and *in vivo* systems. In this section, we summarize the cytotoxic profile of surface functionalized graphene nanomaterials (Table 1).

In 2012, Singh et al. declared for the first time that amine-modified graphene (G-NH_2) obtained from replacing –COOH groups on GO sheets to corresponding –NH_2 groups was the safest and most biocompatible graphene derivative, which could remarkably reverse the cytotoxicity, aggregatory effects and thrombotoxicity of GO [17]. Similarly, Perini and coworkers recently proposed that NH_2-GQDs possessed highest biocompatibility compared to COOH-GQDs and GQDs in terms of cytotoxicity and influence of cell membrane permeability [18]. Even different signaling pathways are activated by amino-functionalized GO compared to GO. The single-cell mass cytometry of human B cells internalized with GO and amino-functionalized GO indicated that amino-functionalized GO differently regulated activation markers including CD38, CD69, CD80, and CD138, and cytokines such as granzyme B. Thus distinctive signaling pathways of B cell receptor and CD40 were induced by GO and amino-functionalized GO for activation of B cells [19].

In case of toxicity to cancer cells, aminated GO with size distribution ranging from 102 nm to 1.944 μm exhibited increased toxicity towards human hepatocellular cancer cells compared to GO with wide size distribution ranging from 280 nm to 6.4 μm [20].

Besides –NH_2 modification, a broad range of natural and synthetic polymers have been successfully modified the surface of graphene nanomaterials via covalent or non-covalent modification in

Table 1
Functionalization of graphene-based materials and biological effects.

Nanomaterial	Modifier	Synthesis	Size (nm)	Biological effects of functionalization	Cell line	Reference
GO	$-NH_2$	Refluxing graphite powder with acidic mixture of sulfuric and nitric acid	2 μm	Decreasing platelet aggregation from 90 % to 8 % at 10 μg/mL, No hemolysis at 50 μg/mL, No cytotoxicity for platelet and THP-1cells at 20 μg/mL, No thrombogenic potential.	Platelets, THP-1	[17]
GQD	$-NH_2$	Commercial	< 10	Increasing cell viability from 80 % to 100 %, No effect on membrane permeability.	U89	[18]
GO	Starch	Modified hummer's	162	<5% hemolysis up to 500 ppm, No cytotoxicity up to 100 ppm.	A549	[22]
GO	CS	Modified hummer's	No data	Decrease hemolysis from 8.6 % to 0.4 %, Increase cell viability from 85.6 % to 96.3 % at 100 μg/mL.	HDF	[23]
MGO	CS-SA	Modified hummer's	500	Stabilizing MGO, Suppressing nonspecific protein absorption, No cytotoxicity at 50 μg/mL.	A549	[24]
GO	SA	Modified hummer's	87	No cytotoxicity up to 400 μg/mL.	Hela	[25]
GO	SA	layer-by-layer (LbL) technique	362	Stabilizing GO, Reducing nonspecific protein absorption, No cytotoxicity at 50 μg/mL.	MCF-7	[26]
GO	Cellulose	Marcano method	No data	No obvious cytotoxicity for Hela and NIH-3 T3 cells at 100 μg/mL.	NIH-3 T3, Hela	[27]
rGO	HA	Commercial	108	Increasing cell viability from 70 % to 100 % for MCF-7 cells at 75 μg/mL, Increasing cell viability from 50 % to 100 % for NHDF cells at 75 μg/mL, Targeting CD44 overexpressed cancer cells.	MCF-7, NHDF	[30]
GO	Heparin	Modified hummer's	119.8	Stabilizing GO, < 3 % hemolysis at 500 μg/mL, Decreasing the pulmonary toxicity.	MCF-7, HepG2	[154]
GO	PEG	Modified hummer's	< 50	Stabilizing GO, No cytotoxicity at 100 μg/mL.	HCT-116	[35]
GO	PEG	Modified hummer's	50–200	Stabilizing GO, No cytotoxicity for A549 and MCF7 at 100 μg/mL.	A549, MCF7	[36]
O-GNR	DSPE-PEG	Oxidative longitudinal unzipping	0.5–2.5 μm	1-fold cellular uptake in U521 cells than MCF7 and GC-4 cells, No cytotoxicity for all three tested cell lines at 80 μg/mL.	MCF-7, GC-4, U521	[37]
GO	PEG	Commercial	300–500	Stabilizing GO, Increasing cellular uptake, cell attachment and proliferation.	MSCs	[38]
GO	PAA	Hummer's	269	Increasing cell viability from 50 % to 100 % at 100 μg/mL, Reducing LgG absorption from 62.2 % to 36.8 %, No inflammation after 14 days exposure.	J774.A1, *in vivo*	[34]
GO	PVP	Modified hummer's	200	Decreasing hemolysis from 50 % to 3.8 %, No cytotoxicity at 100 μg/mL.	MCF-7	[23]
GNP	PVA	Commercial	25 μm	0.05 % hemolysis at 500 μg/mL, Negligible cytotoxicity at 100 μg/mL.	HFF1	[33]
GO	PAMAM	Commercial	80–100	Increasing cytotoxicity from 7 % to 45 % for SMMC-7721 cells at 200 μg/mL, Increasing cytotoxicity from 46 % to 90 % for HEK-293 cells at 200 μg/mL, Promoting gene transfection efficiency.	SMMC-7721, HEK-293	[42]
GO	PAMAM-GA	Commercial	80–100	Stabilizing GO, Increasing gene transfection efficiency, Negligible cytotoxicity for SMMC-7721cells at 200 μg/mL, 30 % cytotoxicity for HEK-293 cells at 200 μg/mL	SMMC-7721, HEK-293	[42]
GO	HP-β-CD	Brodie method	100	Stabilizing GO, 0.2 % hemolysis at 1 μg/mL, No cytotoxicity within 24 h, 20–40 % increase of cell viability at 48 h and 72 h.	Hela	[46]
GO	β-CD	Hummer's	520	26.2 % increase of DOX loading, Increasing cell viability from 70 % to 80 % at 50 μg/mL.	MCF-7	[44]
MGO	PNIPAM-β-CD	Hummer's	410–499	Stabilizing MGO, Increasing DOX loading efficiency, No cytotoxicity for MCF-10A cells at 125 μg/mL, 20 % cytotoxicity for MCF-7 cells at 125 μg/mL.	MCF-7, MCF-10A	[47]
MGO	CDHA	Modified hummer's	338.5	Stabilizing GO, 18 % increase of DOX loading efficiency, Targeted delivery,	BEL-7402	[43]

(*continued on next page*)

Table 1 (*continued*)

Nanomaterial	Modifier	Synthesis	Size (nm)	Biological effects of functionalization	Cell line	Reference
				Negligible cytotoxicity at 40 μg/mL.		
GO	Protein corona	Modified hummer's	No data	Increasing cell viability from 50 % to 90 % at 100 μg/mL.	A549	[49]
GO	Protein corona	–	200–700	Decreasing hemolysis from 80 % to 4 %.	Red blood cells	[50]

CDHA- β-cyclodextrin–hyaluronic acid polymers; GNP- Graphene nanoplatelets; HP-β-CD- Hydroxypropyl-β-cyclodextrin; MGO- Magnetic graphene oxide; O-GRN- Oxidized graphene nanoribbons; PAMAM-GA- Polyamidoamine -glycyrrhetinic acid; PNIPAM-β-CD- Poly *N*-isopropylacrylamide- β-cyclodextrin.

order to develop biocompatible graphene nanomaterials [21]. The most frequently used natural biopolymers are starch [22], chitosan (CS) [23,24], sodium alginate (SA) [25,26], cellulose [27,28], hyaluronic acid (HA) [29–31] and Hep [32]. These biopolymers are favored in fabrication of graphene-based drug delivery systems owing to their non-toxicity, biocompatibility, and biodegradability features, among other excellent properties. It has been well proved that coating graphene nanomaterials with these biopolymers is a brilliant strategy to stabilize, reduce cytotoxicity as well as to enhance biocompatibility of graphene nanomaterials. Particularly, HA functionalization is more ideal than other biopolymers in targeted drug delivery, as it not only possesses the outstanding natures of natural biopolymers, but also specifically targets certain over-expressed receptors on numerous cancer cells [29–31].

In addition, functionalizing graphene nanomaterials with synthetic polymetric molecules such as polyethylene glycol (PEG) [12], polyvinylpyrrolidone (PVP) [23], polyvinyl alcohol (PVA) [33], PAA [34] exhibits desirable effects on improving GO nanomaterials biocompatibility as well. Among which, PEG and PVP are commonly considered as safe polymers since they have been approved by the United States Food and Drug Administration (FDA) for diverse usages in humans. PEG is the most famous and well-studied polymer regarding modification of GO nanomaterials for drug delivery. As illustrated by plenty of literatures, PEG coating contributed to stabilizing GO nanomaterials in physiological environment, promoting cellular uptake of GO, increasing drug loading/releasing behavior and decreasing cytotoxicity [35–38]. Long-term study on distribution and toxicology of PEGylated GO nanomaterials *in vivo* further demonstrated dramatic merits of such functionalization [39,40]. The effect of GO functionalization with PEG with two different structures of linear and branched was recently demonstrated on monocytes of peripheral blood. Interestingly PEG structure determines the GO-PEG uptake by monocytes, and branched PEG could decrease the uptake of GO-PEG by monocytes [41]. Thus, the structure of polymer used for functionalization could determine the uptake of GO functionalized materials.

Positively charged synthetic polymers such as polyethyleneimine (PEI) and polyamidoamine (PAMAM) were also employed for surface modification of GO nanomaterials for the purpose of drug delivery and gene transfection [42]. This is due to that the cationic polymers can easily interact with negatively charged cell membrane and gene molecules. Nevertheless, researchers have concluded that cationic surfaces are more toxic than anionic surfaces, whereas neutral surfaces feature the best biocompatibility [15]. Therefore, more thorough research needs to be done for careful examination of biosafety and biocompatible behavior of cationic coating on GO nanomaterials.

Moreover, small biocompatible molecules modified GO nanomaterials may also have a significant performance in drug delivery systems. For instance, β-cyclodextrin (β-CD), a FDA-approved biocompatible molecule, is very attractive regarding modification of GO nanomaterials in recent decades [16,43]. β-CD composes of a hydrophilic external surface and a hydrophobic internal cavity that endows it not only a good water solubility but also high ability to selectively attract various hydrophobic drugs into their cavity via host–guest interaction [44]. Thus, modifying GO nanomaterials with β-CDs offers an effective way to improve biocompatibility of GO nanomaterials and enhance drug loading efficiency at the same time [43–47].

To address the biopersistence and long-term cytocompatibility of GO nanomaterials, common substrates of natural peroxidases (i.e. horseradish peroxidase (HRP)), such as coumarin and catechol were modified onto GO to accelerate biodegradation of GO [48]. However, more efforts should be taken in this topic since both *in vitro* and *in vivo* results are still lacking.

Furthermore, preformed protein corona on the surface of GO could greatly alleviate the cytotoxicity and hemolytic activity of GO, providing an alternative option to solve the biosafety problem of graphene nanomaterials [33,49,50]. It was demonstrated that protein (FBS) coated GO at 20 μg/mL concentration showed almost no cytotoxicity to human lung A549 cells while 90 % cell viability was observed at high concentration (100 μg/mL) [49]. Moreover, the effect of GO on hemolytic activity could be also greatly reduced by this protein corona effect [50]. In fact, when the surface of GO is occupied by protein corona, the available surface area of GO plus unfavorable steric effect could be reduced, thereby weakening the physical interaction between membrane and GO [51].

In vivo studies: Chemical functionalization is also an appropriate strategy to alleviate graphene-based nanomaterials cytotoxicity *in vivo*. PEG coated GO is less toxic than unfunctionalized counterpart [52]. As evidenced by long term biodistribution studies, PEGylated small nanographene sheets (10–30 nm) do not cause appreciable toxicity on mice treated with 20 mg/kg dose for a period of 3 months [39]. Similarly, GO functionalized with PEG at 184 nm size and 500 pg dosage significantly attenuated the GO toxicity in zebrafish embryos. However, abnormal branching and mispatterning of developing trunk blood vessels were observed by GO and even GO-PEG [52]. Thus, even the GO functionalization would not help in attenuating the angiogenic defects in zebrafish embryos.

Considering worm *in vivo* model system (*Caenorhabditis elegans*), BSA chemically bonded GO sheets (180 nm) prevent acute and prolonged toxicity in primary and secondary organs. GO-BSA at 0.5–100 mg/L did not affect the intracellular redox status and lifespan of *C. elegans* [53]. Thus, GO-BSA can be suggested as a safe GO based drug carrier however, it needs to be further proved in other *in vivo* model systems.

Altogether, versatile biocompatible molecules (Table 1) have been explored to modify GO nanomaterials, reduce the cytotoxicity, and improve the biocompatibility of GO nanomaterials for better drug delivery. However, it is still early to conclude which molecule has the best performance based on the currently available knowledge. But the information provided in this section and in the accompanying table (Table 1) may aid researchers with regard to what type of functionalization, synthesis method, particle

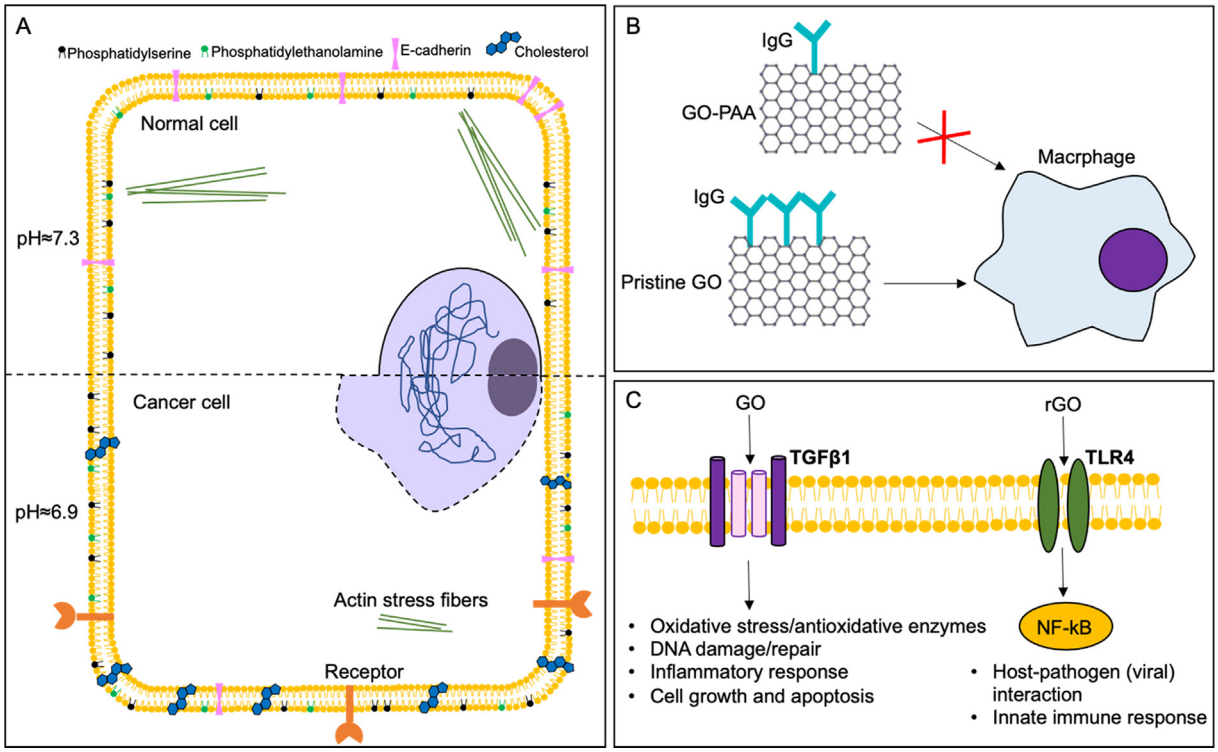

Fig. 1. A) Fundamental differences between normal and cancer cells, and various effects of GO and GO derivatives on bio-molecular processes in B) normal and C) cancerous cells. A) Compared to normal cells, cancer cells have larger nucleus, the nucleus envelope is abnormally perforated and deformed, actin stress fibers are less organized and less dense, the expression of adhesion protein E-cadherin is reduced, phosphatidylethanolamine and are present at high concentrations in the outer leaflet, and increased cholesterol in multi-drug resistant cancer cells turns the membrane being rigid and less permeable for drugs. B) Low serum IgG adsorption by GO-PAA and thereby weak interaction with macrophages compared to GO [34]. C) Distinct signaling pathways affected in response to hydrophilic GO and hydrophobic rGO at the cell surface level/subcellular level [62]. GO-PAA, poly (acrylic acid)-functionalized GO; IgG, immunoglobulin G; TGFβ1, transforming growth factor beta-1 receptor.

size, concentration, and cell lines would be needed to ensure reduced cytotoxicity and improved biocompatibility.

3. Fundamental differences of cancerous versus non-cancerous cells

There are many studies comparing the mechanics of individual normal and cancer cells and they found that the cell stiffness decreases when a normal cell transforms into a cancer cell [54]. Even the stiffness decreases within disease progression. Based on cytoskeletal elements particularly actin distribution and organization, Alibert et al. (2017) summarized the studies showing the individual cancer cells are softer than normal cells and/or the softness correlates with malignancy. Compared to the normal cells, i) cancer cells have larger nucleus, ii) the nucleus envelope is abnormally perforated and deformed, iii) cell adhesion components such as actin stress fibers are less organized and less dense; iv) extra centrosomes with abnormal positioning and elongated shape are appeared; and v) the expression of adhesion protein E-cadherin is reduced (Fig. 1A).

Acidic extracellular pH is a major feature in tumor tissue that is due to lactate secretion from anaerobic glycolysis [55]. This feature affects the cancer cells to rearrange the plasma membrane to adapt the acidic microenvironment. In this case, phosphatidylethanolamine (PE) and phosphatidylserine (PS) that are mainly confined in the inner leaflet of the membrane, are present at high concentrations in the outer leaflet of the cancer cells. Furthermore, altered cholesterol metabolism could lower cholesterol in metastatic cells membrane and enhance deformability, thereby increasing their ability to enter to the blood vessels. While increased cholesterol in multi-drug resistant cancer cells turns the membrane being rigid and less permeable for drugs [56]. Furthermore, there are abundantly expressed receptors on tumor cell surface which makes them an ideal molecular target for targeted delivery of anticancer therapeutics.

It is expected that these fundamental differences between cancerous and non-cancerous cells cause the cancer cells interacting with graphene-based materials in different manners.

4. Interactions of graphene-based materials with mammalian cells

GO and its derivatives affect the expression of protein coding genes and microRNAs (miRNAs), as well as structure and behavior of proteins, sub-cellular cellular structures (cytoskeleton, membranes) and entire organelles and compartments (mitochondria, lysosomes, nucleus, endoplasmic reticulum (ER), and peroxisome). In this section, we describe the interactions of graphene-based materials with bio-molecular processes, plasma membrane, cytoskeleton, membrane organelles including lysosome, mitochondria, nucleus, ER, and peroxisome in normal and cancer mammalian cells (Table 2).

4.1. Interactions of graphene-based materials with bio-molecular processes

4.1.1. Distinct protein corona profile response to different graphene-based nanomaterials

Due to the high surface free energy, nanomaterials are rapidly coated by proteins in biological matrices forming a “protein corona”. This coating can make them visible to be uptaken by immune cells. Proteome studies were conducted to explore this protein cor-

Table 2
The effect of graphene-based materials on different parts in the cells.

Interaction site	Nanomaterial	Synthesis	Particle size (nm)	Cell line	Biological effects	Reference
Transcriptome	GO, rGO	Commercial	40	Liver carcinoma cell	Similar totoxicity, DNA damage, oxidative stress for GO and rGO GO with cellular uptake, NADPH oxidase dependent ROS formation, high deregulation of antioxidant/DNA repair/ apoptosis related genes TGF-β1 mediated signaling in GO induced biological/toxicological effect rGO adsorbed at cell surface without internalization, ROS generation by physical interaction, poor gene regulationrGO elicited host-pathogen (viral) interaction and innate immune response through TLR4-NF-kB pathway	[62]
Transcriptome	GO	Exfoliation of graphite oxide	50	Embryonic kidney cell	Dose-dependent cytotoxic effect on HEK293 cells Increased LDH leakage, ROS generation, decreased GSH, increased oxidized glutathione indicative of oxidative stress Decrease in mitochondrial membrane potential and ATP synthesis, DNA damage and caspase 3 activity Altered expression of multiple apoptosis-related biological pathways genes, key transcription factors promoting the apoptosis-related pathways by regulating their downstream genes	[155]
Transcriptome	GO, GO-NH_2, GO-PAM, GO-PAA, GO-PEG	Hummer's	GO 201, GO-NH2 251, GO-PAM 363, GO-PAA 269, GO-PEG 272	Murine macrophage cell Male BALB/c mice	Pristine GO impaired cell membrane integrity and regulation of membrane- and cytoskeleton-associated genes, membrane permeability, fluidity and ion channels GO induced platelet depletion, pro-inflammatory response, pathological changes of lung and liver in mice GO-PAA less toxicity than pristine GO, the most biocompatible one due to the differential compositions of protein corona	[34]
miRNA	GO	Modified hummer's	51	Pulmonary adenocarcinoma cells	Reduced cell viability, induction of LDH leakage, ROS production, apoptosis, and dysregulation of cell cycle Localized in cytosol, mitochondria, endoplasmic reticulum, and nucleus of cells Dysregulated miRNAs activate both a death receptor pathway by influencing functions of tumor necrosis factor R receptor, caspase-3 and mitochondrial pathway by affecting functions of p53 and Bcl-2	[96]
miRNA	GO	–	–	Lung carcinoma cell	Affected adherens junction, focal adhesion, TGF-β1 signaling pathway MiRNA targeting of genes (Rac1 and RhoA) involved in the cytoskeleton assembly process	[63]
Proteomics	GO-PEG	Hummer's	100–200	Breast cancer cell, mammary epithelial cell, mouse embryonic fibroblast cell	Impaired mitochondrial OXPHOS in breast cancer cells but no effect on that in non-cancerous cells Down-regulated PGC-1α in breast cancer cells, modified expression of energy generation-related proteins for the inhibition of OXPHOS Reduced ATP production and impaired assembly of F-actin cytoskeleton in breast cancer cells	[11]
Proteomics	GO	Commercial	300–500	Lung carcinoma cell	Toxic effects on cells by regulating gene transcription, immune response, cell growth, apoptosis SMARCA4, TGF-β1, and TP53 as key node proteins regulating GO toxicity	[64]
Proteomics	SLGO, MLGO	Commercial	SLGO 176.9, MLGO 467.9	Fetal bovine serum	SLGO enriched FBS proteins involved in metabolic processes and signal transduction MLGO enriched proteins involved in cellular development/structure, and lipid transport/metabolic processes	[57]
Plasma membrane	GO	Modified hummer's	51	Lung cancer cells	Reduction in cell viability, induction of LDH leakage, ROS production, apoptosis, dysregulation of cell cycle	[96]
	Graphene-gambogic acid	Using an radio frequency generator, purified with HCl	100–200	Breast and pancreatic cancer cells	LDH release, mitochondria dehydrogenase activity, mitochondrial membrane depolarization, DNA fragmentation, intracellular lipid content, membrane permeability/caspase activity	[130]
	GO, carboxyl graphene nanoplatelets	Modified hummer's	100–300	Liver cancer cell	Increased intracellular ROS, alterations in cellular ultrastructure, changes in metabolic activity	[69]
	Pristine GO, rGO, hGO	Modified hummer's	321.5, 456.5, 340.8	Epithelial cells, macrophages, murine lung cells, mice	Lipid peroxidation of surface membrane, membrane lysis, cell death, acute lung inflammation, highest lipid peroxidation in alveolar macrophages, cytokine production (LIX, MCP-1), LDH release in bronchoalveolar lavage fluid	[93]

Table 2 (*continued*)

Interaction site	Nanomaterial	Synthesis	Particle size (nm)	Cell line	Biological effects	Reference
Cytoskeleton	GO-PEG	Modified hummer's	10–120	Human osteoblasts, preosteoblasts, macrophages	Localizing on F-actin filaments, inducing cell-cycle alterations, apoptosis, oxidative stress	[99]
	GO-doxorubicin, cisplatin	Modified hummer's	100–300	Macrophages, lung cancer cells	Compromising plasma membrane and cytoskeleton, suppressed integrin expression	[102]
Lysosome	GO quantum dots	Commercial	41	Immortalized mouse spermatogonia and mouse Sertoli cells	Inhibiting lysosome proteolytic capacity	[103]
	GO	Commercial	439	Rat pheochromocytoma cells	Blocking autophagic flux, disrupting lysosome degradation, caspase 9-mediated apoptosis	[104]
Mitochondria	rGO	Hummer's	200	Breast cancer cell	Inhibited proliferation of MCF-7 cells, mitochondrial-mediated programmed cell death with involvement of the NF-kB signaling pathway	[111]
	GO-ZnO	Using an radio frequency generator, purified with HCl	62	Human breast cancer cell	ROS production	[130]

GO- Graphene oxide; GO-NH_2- Aminated GO; GO-PAA- poly(acrylic acid)-GO; GO-PAM- poly(acrylamide)-GO; GO-PEG- poly-(ethylene glycol)-GO; GSH- reduced glutathione; hGO- hydrated GO; LDH-lactate dehydrogenase; miRNAs- MicroRNAs; MLGO- multi-layered GO; OXPHOS- oxidative phosphorylation; rGO- Reduced graphene oxide; ROS- Reactive oxygen species; SLGO- Single-layer GO.

ona that forms around GO upon exposure to plasma and serum [57,58]. 394 proteins were detected in hard corona composition of single layer GO (SLGO) while 290 were found on the multi-layered GO (MLGO). Among these proteins, SLGO exclusively coated with 115 proteins involved in signal transduction and metabolic processes, and MLGO with only 11 proteins that involved in lipid transport/metabolic processes and cellular development/structure [57]. It was concluded that the surface area and chemistry as well as aggregation could determine the protein corona profile on GO nanomaterials. Moreover, Di Santo et al. (2020) showed minor impact of lateral size on protein corona composition [58]. Similarly, Ekal et. al., (2022) demonstrated that the interactions of GO with proteins such as BSA could be modulated by the extent of oxidation on GO sheets [59].

Interestingly, GO functionalization with PEG, polyacrylic acid (PAA), and D-mannose diminished the serum protein adsorption to the GO. Especially the adsorption of immunoglobulin G (IgG) was reduced, leading to a weaker interaction of functionalized GO with macrophages [34,60] (Fig. 1B). The authors concluded that such functionalized GO derivatives are less toxic and "invisible" to the immune system, leading to longer systemic circulation and thereby higher delivery to the target sites.

Human proteome changes in several types of cancer, that can be used for early cancer detection. Depending on changes in human proteome, protein corona with different composition could be formed around GO upon exposure to human plasma, that can be used as the *in vitro* diagnostic tool. However, Di Santo et al., (2020) demonstrated that the GO lateral size (100, 300, and 750 nm) had a negligible effect on the composition of protein corona [61].

Overall, we conclude that the number of layers, oxidation degree, and functionalization can be considered as the critical factors determining the protein corona profile on GO nanomaterials as well as invisibility of GO carriers to the immune system.

4.1.2. Distinct signaling pathways affected in responses to different graphene-based nanomaterials in cancerous cells

The surface chemistry of Graphene-based nanomaterials affects the biomolecular response of cells. The surface chemistry including oxidation (O/C ratio) modulates hydrophilicity/hydrophobicity of GO/ reduced graphene oxide (rGO), which in turn governs their interactions with the living cells and their components. The differential gene expression analysis of HepG2 (human liver carcinoma cells) after 24 h of treatment with hydrophilic GO (20 μg/mL) revealed that 1224 genes were 1.5-fold induced or repressed. By contrast, the hydrophobic rGO with the same lateral size distribution (40 nm) at EC20 dose (8 μg/mL) under similar conditions of treatment of the same cell line induced or repressed much fewer genes, only 297 [62]. GO was found to affect the transcription of genes mostly involved in the cell cycle, response to DNA damage, regulation of cell growth and apoptosis, response to oxygen stress and hypoxia, regulation of intracellular transport, that mediated by the active transforming growth factor beta-1 (TGFβ1) receptor signaling pathway (Fig. 1C) [62–64]. rGO treatment affected a different subset of genes, those mostly involved in the cell surface receptor-linked signal transduction, virus-host interaction, and immune response, that mediated by toll-like receptor (TLR4-NF-κB) signaling pathway. Therefore, hydrophilic GO interacts with TGFβ1 receptor while hydrophobic rGO interacts with Toll-like receptor, that subsequently affect different downstream mechanisms inside the cells.

Therefore, we can target different intracellular signaling pathways in cancerous cells by engineering the surface chemistry of GO nanomaterials.

4.2. The effects of graphene-based nanomaterials on the plasma membrane

Based on the particle size and surface chemistry, the internalization of graphene into cells via endocytosis can occur through different types of processes: clathrin-mediated endocytosis, caveolae-mediated endocytosis, macropinocytosis, phagocytosis, and physical penetration [65–68].

4.2.1. Size-dependent effects of graphene-based nanomaterials on plasma membrane in normal cells

The size of GO nanomaterials is a key parameter which influences their impact on plasma membrane internalization and toxicity (Fig. 2A-H). Mu et al., (2012) demonstrated the size-dependent internalization of protein-coated GO nanosheets by mouse mesenchymal progenitor C2C12 cells. The largest GO platelets (860 nm) were retained by the microvilli and they were not inter-

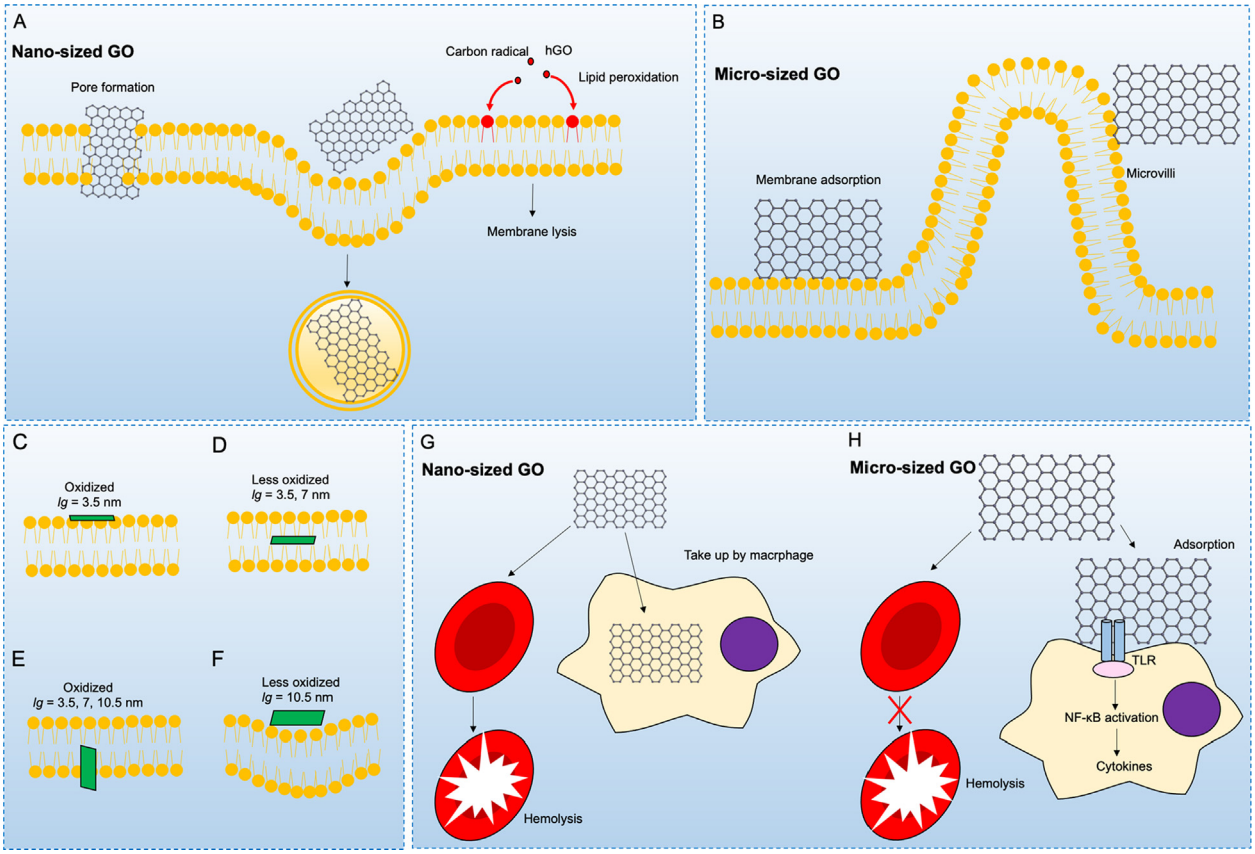

Fig. 2. The underlying mechanism for GO interaction with plasma membrane in normal cells. A) Nano- and B) micro-sized GO interaction with plasma membrane [66]. C-F) Side length and oxidation-dependent internalization of graphene nanosheets [68,73]. G) Biocompatibility of nano-sized and H) micro-sized GO for plasma membrane [76]. hGO, hydrated GO.

nalized (Fig. 2B) [66]. In another study, largest nanosheets (860 nm) were internalized by phagocytosis. Smaller nanosheets (420 nm) were internalized by clathrin-mediated endocytosis. Finally, the smallest nano-sized (100 to 300 nm) platelets were observed to be deposited onto the flat plasma membrane domains without microvilli, but no uptake into endocytosis vesicles was detected in this study [69]. Thus, 400–900 nm sized GO particles get inside the cell but smallest one could not get inside.

Mendes et al., (2017) tracked the endocytosis of GO flakes with different diameter distributions (453, 277, 46 nm) within different incubation periods in undifferentiated human monocyte and differentiated macrophage cells. Interestingly, GO uptake starts rapidly within 2 min. The uptake rates are size dependent for both types of cells as larger flakes (or clusters of flakes) could be easily internalized compared to small individual flakes [70]. In another study, the effects of GOs with two different lateral sizes (91 and 583 nm) but similar physicochemical properties were indicated on three different major cell types of liver (Kupffer cells (KCs), liver sinusoidal endothelial cells (LSECs), and hepatocytes) [71]. GOs showed significant toxicity to Kupffer cells compared to other cell types of liver, which is due to higher uptake or cell association with plasma membrane. Furthermore, GO induced lateral size-dependent toxicity to Kupffer cells with higher uptake of large sized GO and thereby higher toxicity to Kupffer cells than small sized GOs. Thus, differential toxicity of GO was demonstrated to different cell types of liver. In fact, the majority of GOs was swallowed by Kupffer cells through phagocytosis while LSECs and hepatocytes could only uptake GO through clathrin-mediated endocytosis with 200 nm size limit that were not able to uptake large sized GO. Hence, it can be concluded that various mechanisms of cellular uptake significantly impact the cytotoxicity of GO.

The GO with various sizes (large size: 10–40 μm and small size: 50–300 nm) could cause lipid perturbations in the plasma membrane of primary human neutrophils. Specifically, lipid raft domains in neutrophils were effectively disrupted by large GO sheets compared to the small GO and this disruption triggered neutrophil extracellular traps (NETs) [72]. Furthermore, high doses of single-layered GO like 200 μg/mL with diameter of 200–700 nm could form pores in the plasma membrane of human lung A549 and murine Raw 264.7 macrophages cell lines [68] (Fig. 2A). Increasing nanosheet edge length also could enhance the perturbation degree of membrane. Mao et al., (2014) showed densely oxidized graphene nanosheet with side length *lg* = 3.5 nm adheres to the top surface of the membrane (Fig. 2C). The graphene-sandwiched superstructure by pristine graphene nanosheet with side length *lg* = 7.0 nm was hosted inside the lipid bilayer (Fig. 2D) that seems to be difficult to internalized through the endocytosis. Meanwhile, pristine graphene nanosheet with increased *lg* (10.5 nm) was encapsulated by the hemisphere vesicle of lipids extracted from the membrane [73] (Fig. 2F). Thus, the lateral dimensions, side length, and doses of graphene-based nanomaterials need to be optimized for drug delivery to minimize the membrane perturbation.

The size of GO nanomaterials can also influence the intracellular fate of GO. The exposure of micro-sized GO (750–1300 nm) at 20 μg/mL for 6 h was prone to plasma membrane adsorption (Fig. 2B). It activated the toll-like receptors (TLRs), M1 polarization and nuclear factor NF-κB to produce pro-inflammatory cytokines *in vitro* (Fig. 2H). GO administration into the abdominal cavity, lung, or bloodstream through the tail vein of BALB/c male mice was shown to develop inflammatory responses *in vivo*. Whereas smaller sized ones (50 to 350 nm) at same concentration and expo-

sure time retained higher potential for biocompatibility and cellular uptake by macrophages that defend at the portal-of-entry against foreign agents and release substances to activate other immune cells (Fig. 2G) [74]. Therefore, nano-sized GO (50 to 350 nm) is suggested as a suitable carrier in terms of avoiding inflammation response. In agreement with this result, medium sized GO (321.74 nm) appeared as a least harmful to the human embryonic kidney cells, meanwhile small GO (31.25 nm) caused the highest cytotoxicity even at low concentration (5 mg/L), and large GO especially at a higher concentration (100 mg/L) could elevate cell death [75]. The severe impacts caused by large size GO at high dose and extended exposure could possibly related to the physical damages by cells adsorption, while the significant cytotoxicity of small size GO even at the lower concentration could be due to internalization.

There are several studies showing the micro-sized graphene is more biocompatible. Upon nanomaterial administration, red blood cells (RBCs) are one of the primary sites of interaction. Nano-sized GO (340 nm) at 25 μg/mL could induce 70 % of hemolysis after 3 h exposure compared to the micro-sized (3 μm) graphene sheets, which caused 10 % of hemolysis at 100 μg/mL [76] (Fig. 2G, 2H). The serious disruption in human erythrocyte membrane by nano-sized GO could be attributed to strong electrostatic interactions between the negatively charged GO surface and the lipid bilayer. By contrast, the relatively low toxicity of micro-sized graphene sheets may have been due to their lower overall surface areas. In another study, graphene nanoplatelets with 1–2 μm size was more biocompatible than larger ones (5 μm) in human fibroblasts [77]. Likewise, the submicro-sized GO (390 nm) and nano-sized GO (65 nm) but not the micro-sized GO (1090 nm) could significantly induce apoptosis associated with autophagy while causing no detectable necrosis in vascular endothelial cells [78].

The aggregated carbon nanomaterials (micro-sized graphene sheets), wide size distribution (10–800 nm), proper surface coating (chitosan, bovine serum albumin (BSA), and heparin (Hep)), pH-responsive conformational changes and thereby aggregation, addition of 1 % Tween 80 surfactant could reduce the aggregation of blood cells and increase the hemocompatibility of graphene [76,79–81]. It is interesting to know that once GO is functionalized with PEG, the PEG-GO with different sizes of 100–200 nm and 1–5 μm had no or negligible effect on the viability of cells and the particle size could not significantly affect the cytotoxicity of functionalized nanomaterials [41]. Thus, the cytotoxicity effect of particle size could be only limited to non-functionalized GO.

In vivo studies: The occurrence of oxidative stress and the induction of apoptosis are demonstrated in fish larvae exposed to all different-sized GO particles (50–200 nm, <500 nm, >500 nm) [82]. Then, broad size range of 50–500 nm GO can cause apoptosis in fish larvae.

Graphene derivatives with various lateral size, including GO (115 nm), rGO (107 nm), GO quantum dots (GOQD) (39 nm), and GQD (35 nm) are evaluated in mice. GO and rGO with larger size rather than GQD and GOQD, caused significant toxicity *in vivo*. The GO and rGO could easily absorb proteins and aggregate in the blood, followed by platelet activation to clot and triggering immuno-inflammatory responses. Furthermore, it could mainly block the lung blood vessels, which induced pulmonary histopathological changes consisting of the formation of pulmonary bullae and widened alveolar septa while hepatic and renal function were also impaired. However, GQD and GOQD with small particle sizes and no aggregation within capillaries, showed no obvious toxic side effects *in vivo* [83]. Thus, GQD and GOQD are proposed as the safe materials for designing drug carrier.

Overall, small sized GO with<100 nm could show highest cytotoxicity even at low concentration, while microsized GO (1–3 μm) at high dose and long exposure could cause physical damages. However, the cytotoxicity effect of particle size comes from the mechanism of their uptake that varies among different cell types. Furthermore, the cytotoxicity effect of GO size would be matter only when GO is non-functionalized, thus, we could get rid of size effect by functionalization.

4.2.2. Surface chemistry-dependent effects of graphene-based nanomaterials on plasma membrane in normal cells

The surface chemistry of GO nanomaterials is another key parameter which influences their impact on plasma membrane internalization and toxicity. Chen et al. (2016) demonstrated that the dynamics simulation of GO and pristine graphene with same sizes (Small size: 2.1 × 2.1 nm^2, Middle size: 3.1 × 4.1 nm^2, Large size: 3.7 × 5.4 nm^2) showed no effect of pristine graphene on the membrane integrity while it could readily penetrate into the bilayer. This would be different in case of GO that embedded in the membrane, several membrane lipids are pulled out to the GO surface, followed by pore formation and water flow into the membrane. GO's oxygen-containing groups and strong dispersion interactions between hydrophobic domains and the lipid tails of the bilayer are speculated to enhance the adsorption of lipids on the GO surface [84]. As it was recently reviewed by our group, the strong adhesion of phospholipids to graphene materials with proper oxidation degree (not too less or too much oxygenated groups) could overcome the hydrophobic packing of phospholipids, that causes lipid extraction from the cell membrane onto the graphene nanosheet and thereby a deeper penetration into the cell membrane [85–87]. But there is no report on such GO interaction with phospholipids in mammalian cells. However, computational study and the results of study on two mammalian cell lines including neurons and fibroblast NIH-3 T3 cells support the cholesterol extraction by graphene materials from cell membrane that may cause loss of membrane integrity and cytotoxicity of graphene materials [88,89]. Although the role of graphene materials surface chemistry with the extraction was not reported.

Tu et al., (2017) demonstrated that the uptake was found for the positively ($-NH^{3+}$) and negatively ($-OSO^{3-}$) charged graphene sheets, while no significant uptake was shown for the neutral analogs. Furthermore, the efficacy of positively charged graphene sheets uptake is size independent and occurs mainly through phagocytosis and clathrin-mediated endocytosis pathways. However, the efficacy of negative charge graphene sheets uptake is size dependent, and occurs mainly through phagocytosis and sulfate-receptor-mediated endocytosis [90]. These findings suggest that the impact of GO size on the internalization highly depends on the surface charge.

During the internalization of large size edge GO nanosheets, hemisphere vesicle structure was shown due to the hydrophobic interaction between lipid tails and unoxidized graphene. Small size nanosheet (<4 nm) of either sparsely or densely oxidized graphene completely anchors on the membrane surface due to the strong hydrophilic interaction. Irregular membrane perturbation at large scale and the possible leakage is induced by larger graphene nanosheet (>4 nm) with higher oxidization degree (40 % for basal carbon atoms), destroying the integrity of the membrane. Increasing the basal oxidization degree is expected to favor the graphene nanosheet orientation lying flat on the surface of the membrane and thereby the lipid head groups can be in contact with the oxidized edges to a larger extent. With increasing oxidization degree and from an energy perspective, graphene nanosheets could pierce the membrane with the vertical configuration to the membrane [73] (Fig. 2E). Thus, a larger size (4–10.5 nm) and more oxidized graphene nanosheets (40 % oxidization degree) lead to stronger cytotoxicity.

The nanomaterial dispersion in water or cell culture medium is generally affected by increased surface oxygen. Highly dispersed

graphene may enter the cells in the form of individual flakes rather than as more cytotoxic aggregates [91].

GO (~54 % content of oxygen) and low-reduced GO (~37 % content of oxygen) reduce the viability of cardiac cells at IC50 of 652.1 ± 1.2 and 129.4 ± 1.2 μg/mL, respectively. Therefore, the cell viability of GO and low-reduced GO-treated cells was found to be determined by the surface chemistry of the materials used for treatment, including the numbers of oxygen functionalities, graphitic domains, and particles sizes [92]. Related to the effect of oxidation on biocompatibility, Pinto et al., (2016) demonstrated that graphene nanoplatelets (5 μm) oxidized with ratio 1:6 (with 24 % oxygen content) at concentrations up to 100 μg/mL neither decreased the metabolic activity nor damaged the cell membrane during treatments lasting up to 72 h. The authors argued that the complete oxidation of graphene nanoplatelets folds its sharp edges, thereby assuring biocompatibility. Generally, oxidation status was found to be more important than particle size, since more oxidized graphene nanoplatelets (1:6) have better performance than smaller ones (1–2 μm) with lower oxidation in human fibroblasts [29]. However, this result is in contradiction with previous simulation study showing larger size and more oxidized graphene nanosheets lead to stronger cytotoxicity. Inconsistency can be explained by different size range used in these studies, simulation study examined up to 10.5 nm size, however, this study explored quiet large graphene nanoplatelets of 5 μm.

Critical role of surface functional groups, including carbon radicals, was found impactful on GO biocompatibility in lung (Li et al., 2018). Carbon radicals are more reactive due to the presence of unpaired electrons generating superoxide radicals thereby oxidizing unsaturated lipids and thiol groups on proteins or glutathione (GSH). Hydrated GO (hGO) (340.8 nm) with highest carbon radical density (8.38×10^5), was identified to be responsible for cell death in macrophages and epithelial cells as a consequence of lipid peroxidation of the surface membrane and thereby membrane lysis (Fig. 2A). In contrast, pristine GO (321.5 nm size, 1.85×10^5 carbon radical density) was less toxic, while rGO (456.5 nm size, 0.01×10^5 carbon radical density) showed extensive cellular uptake with minimal effects on viability [93].

In vivo studies: The surface chemistry of graphene-based materials affects their toxicity *in vivo*. Toxicity of various materials with oxidation state (GO (115 nm), and GOQD (39 nm)) and reduction state (rGO (107 nm) and GQD (35 nm)) were compared. rGO was less cytotoxic compared with GO because rGO could easily aggregate in medium due to lack of oxygen-containing functional groups thereby reducing the covering area on the cell surface and adsorption of substances such as proteins and gene. However, oxidation state GOQD and reduction state GQD with small sizes (35–39 nm), dispersed well and rarely covered the cell surface to restrict the nutrient availability [83]. Thus, no significant toxicity was shown for both oxidation and reduction states suggesting that particle size is more important than redox state to affect cytotoxicity.

Appropriate surface modification can also affect the toxicity, as the order of toxicity in *C. elegans* was graphene nanoplatelets pristine (<4 nm) > graphene nanoplatelets-NH_2 (<3 nm) > graphene nanoplatelets-COOH (<3 nm) [94]. However, surface groups such as amino, carboxyl, and hydroxyl (GQD, GQD-NH_2, and GQD-COOH) with 26–40 nm size had no obvious effect on toxicities in mice [83].

Therefore, the surface chemistry of GO nanomaterials greatly affects their interaction with the plasma membrane, and it could determine the internalization process and toxicity in mammalian cells.

4.2.3. Size-dependent effects of graphene-based nanomaterials on plasma membrane in cancer cells

GO showed high affinity towards the plasma membrane and even at concentrations as low as 4 μg/mL caused structural damage in cancerous cells [69,95]. Dynamics and integrity of the plasma membrane could be altered by the GO to induce cancerous cell death [96,97]. LDH leakage measurement is used to assess damage to the membrane. As 48 h exposure with>50 mg/L of GO (51 nm) resulted in severe reduction in cell viability following the induction of LDH leakage from lung cancer cells [96,97]. Thus, GO itself can reduce the viability of cancerous cells through the interaction with plasma membrane.

The chemically engineered cancer cells with membrane proteins conjugated with oligonucleotides were used to determine the interaction of large sized GO with the oligonucleotides on the plasma membrane of cancer cells. Transcriptome analysis of these cells spatially confined with GO showed significant changes in the expression of the MAPK signaling pathway genes that are closely correlated with pseudopods growth and regulation of microfilament skeleton rolling cycle during cell invasion and migration [98]. Thus, interaction of GO with plasma membrane inhibited MAPK signaling pathway followed by inhibition of pseudopods growth and metastasis.

A novel treatment for tumor metastasis was designed based on the interaction of large size GO with the DNA-engineered plasma membrane of cancer cells. In this method, large sized GO was used to cover the cancer cells spatially, blocking the interaction of membrane proteins and external ligands and their downstream pathways and thereby it greatly inhibits metastasis in cancer cells [98].

Altogether, large sized GO itself could beneficially interact with the membrane in cancer cells and inhibits metastasis. It can be directly through blocking the interaction of cancer cells with surroundings and/or indirectly through the inhibition of MAPK signaling pathway.

4.2.4. Surface chemistry-dependent effects of graphene-based nanomaterials on plasma membrane in cancer cells

The GO nanomaterials size and surface chemistry can determine membrane internalization and adsorption in cancer cells. Upon endocytosis inhibitors pretreatment, viability of GO (297 nm, O/C atomic ratio 0.389) treated liver cancer cells with respective EC50 were significantly rescued, while no effect was displayed on viability of the cells exposed to rGO (~36 nm, O/C atomic ratio 0.140) [62]. Thus, hydrophilic GO with larger size and higher O/C atomic ratio was internalized by endocytosis as well as by macropinocytosis, while hydrophobic rGO with smaller size and lower O/C atomic ratio was mostly not internalized and it was only adsorbed at the cell surface. Differential surface chemistry of GO and rGO (especially oxidation status) could also modulate their dispersibility and affect their mode of uptake. Distinct biological and molecular mechanisms of TGFβ1 mediated signaling are induced by hydrophilic GO while the innate immune response through TLR4-NF-κB pathway is induced by hydrophobic rGO in human hepatoma HepG2 cells. NADPH oxidase dependent reactive oxygen species (ROS) formation and high deregulation of antioxidant/DNA repair/apoptosis related genes was demonstrated by GO cellular uptake. Meanwhile rGO was mostly adsorbed at cell surface without internalization, that elicited host-pathogen (viral) interaction and induced ROS formation by physical interaction, and impaired gene regulation [62].

Therefore, engineering the surface chemistry and oxidation degree of GO nanomaterials could be found as a useful strategy to target GO internalization or adsorption on the cell surface in cancer cells.

4.3. The effects of graphene-based nanomaterials on cytoskeleton

4.3.1. The effects of graphene-based nanomaterials on cytoskeleton in normal cells

Cytoskeleton is one of the key cellular components interacting with GO and GO-related nanomaterials directly or indirectly through the cytoskeleton-related genes (Fig. 3A) [45].

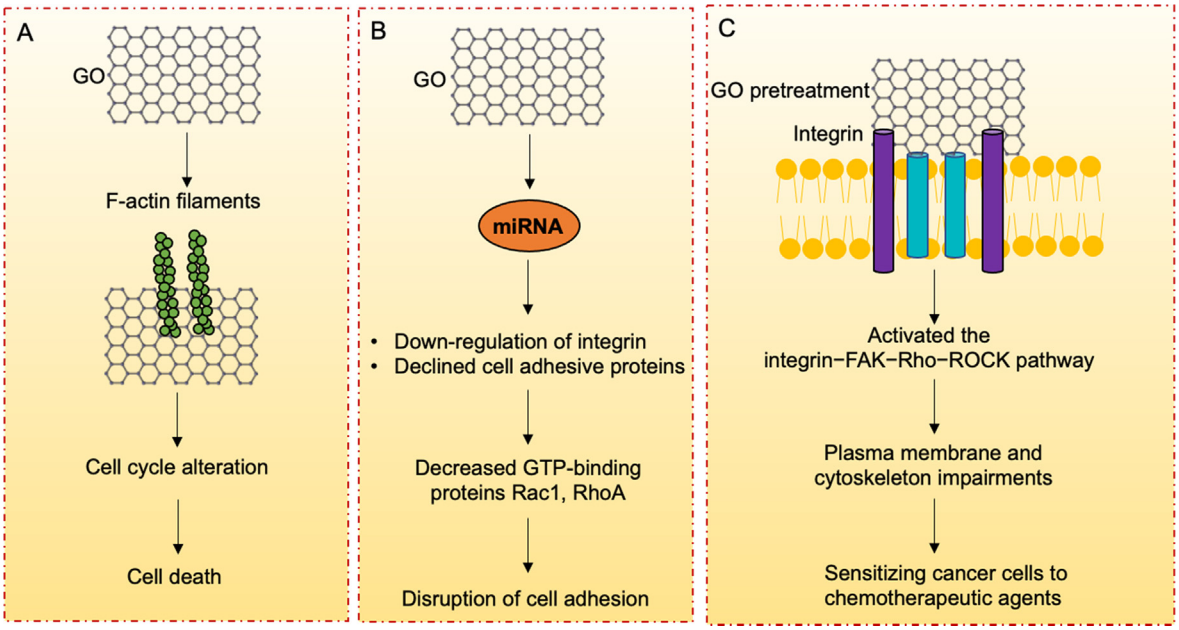

Fig. 3. The mechanism of GO functions in cytoskeleton impairments in A) normal and B-C) cancerous cells. A) GO nanosheets could localize on F-actin filaments and induce cell death [45]. B) Cell adhesion is disrupted through the miRNAs in response to GO [63]. C) Interaction of GO and integrin on the plasma membrane enhances the efficacy of chemotherapeutic agents [46]. MiRNAs, microRNAs.

GO nanosheets (10–120 nm) after their internalization were found to localize on F-actin filaments of osteoblasts, and thus induce alterations in cell cycle and cell death in a cytoskeleton-dependent manner [99]. Therefore, GO nanosheets with<120 nm size could cause cell death through cytoskeleton. This is consistent with significant cytotoxicity of small size GO (31.25 nm) even at the lower concentration (5 mg/L) that was due to the membrane internalization [75]. Pristine GO (201 nm) at low concentration (4 μg/mL) for 24 h was also demonstrated to impair cell membrane integrity by regulation of membrane- and cytoskeleton-associated genes, including Actg2, Myosin, Tubb2a, and Nebulin in Murine macrophage cell line J774A.1 [34].

It can be suggested that the interaction of small sized GO (<120 nm) with cytoskeleton could induce cell death in normal cells.

4.3.2. The effects of graphene-based nanomaterials on cytoskeleton in cancer cells

GO can disrupt cytoskeleton assembly in cancer cells. Tubulin, the key molecule for microtubules, is essential for proliferation and cellular function. GO could disrupt the integrity of the tubulin structure followed by retardation of polymerization. Thus, disruption of microtubule caused growth arrest at the S phase and ROS induced apoptosis in human colon cancer HCT116 cells [100]. It was also shown that alterations in the organization of microtubules and microfilaments and morphological changes could be found when the cells are internalized with the GO and GO derivatives. However, the morphology could be recovered after additional 24 h in normal medium [101].

MiRNAs are a large class of short noncoding RNAs acting to post-transcriptionally inhibit gene expression. The role of miRNAs in regulation of GO toxicity has been previously demonstrated in cancer cells [63,96]. 653 miRNAs were differentially expressed in GLC-82 lung cancer cells treated with 100 μg/mL GO for 48 h. The GO treatment dysregulated miRNAs that activate both a death receptor pathway (through the tumor necrosis factor R receptor and caspase-3) and a mitochondrial pathway (through the p53 and Bcl-2) [96]. Therefore, dysregulated miRNAs could explain the GO toxicity at the molecular level. MiRNAs disrupt the cell adhesion in response to exposure to GO. That is accomplished by down-regulating integrins, cell adhesive proteins (laminin, fibronectin, focal adhesion kinase (FAK; PTK2 protein), cell cycle protein cyclin D3 and GTP-binding proteins such as Rac1 and RhoA [11,63] (Fig. 3B).

GO (100–300 nm) treatment at sublethal concentrations to macrophages (4 μg/mL) and lung cancer cells (10 μg/mL) was shown to compromise plasma membrane and cytoskeleton meshwork and thereby sensitizing cancer cells to chemotherapeutic agents (e.g., doxorubicin (DOX) and cisplatin). Interaction of GO and integrin on the plasma membrane activated the integrin – FAK – Rho – ROCK pathway followed by suppressed expression of integrin, plasma membrane injuries, and cytoskeletal damages [102] (Fig. 3C). Thus, benefit of GO pretreatment could enhance the efficacy of chemotherapeutic agents in killing cancer cells.

Altogether, GO itself could disrupt cytoskeleton assembly that can be beneficial to suppress the cancer cells migration and metastasis.

4.4. The effects of graphene-based nanomaterials on membrane organelles

4.4.1. The effects of graphene-based nanomaterials on lysosome in normal cells

Cytoplasmic materials including nanomaterials engulfed in double-membrane vesicles finally reach to lysosomes for degradation through the autophagy process. The basal level of autophagy is important in maintaining cellular homeostasis, while defective autophagy has been associated with some diseases. Dysfunction of autophagy is considered as a toxicity mechanism of nanomaterials. Autophagic flux could be disrupted by GO and it could cause autophagosome accumulation (Fig. 4A) [103,104]. Autophagic flux was blocked by graphene oxide quantum dots (GOQDs) (41 nm, 100 μg/mL). GOQDs decreased amount and activity of lysosomal cathepsin B enzyme, and inhibited lysosome proteolytic capacity in cell lines derived from immortalized mouse spermatogonia

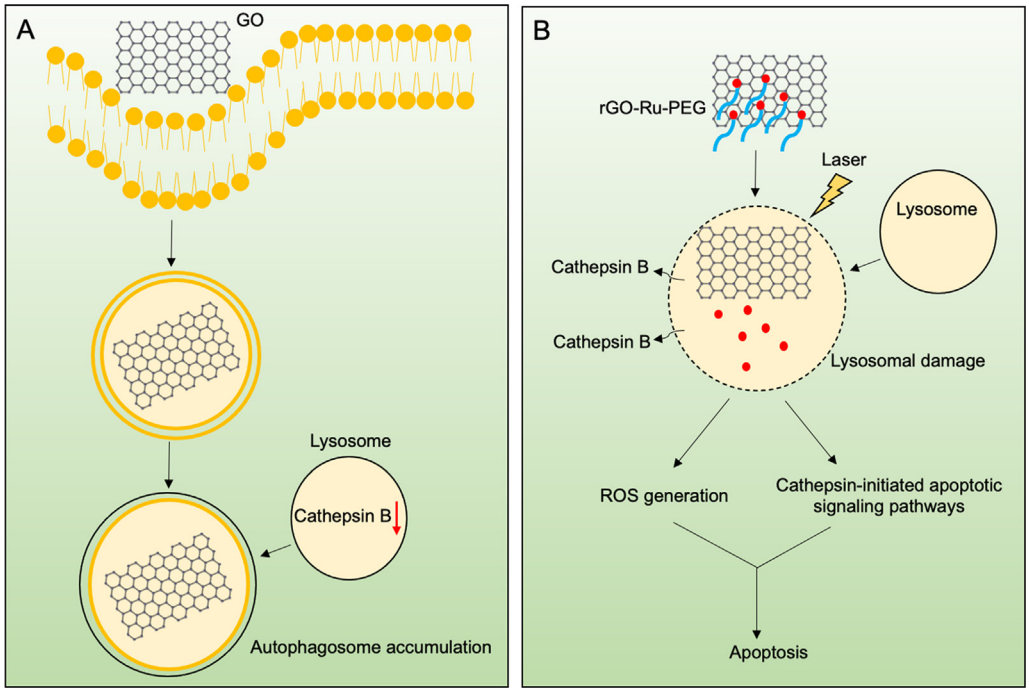

Fig. 4. The interaction of GO with lysosome in A) normal and B) cancerous cells. A) Lysosomal dysfunction and autophagosome accumulation by GO [104]. B) Protonation/deprotonation process of carboxyl groups on rGO in lysosome for the pH-dependent drug release [106].

and mouse Sertoli cells [103]. Consistent exposure of GO (439.14 nm, 60 μg/mL) could induce apoptosis through impairing autophagic flux and lysosomal dysfunction in rat pheochromocytoma cells [104].

Therefore, GO could impair the autophagic flux and lysosome proteolytic capacity through the interaction with lysosomes in normal cells.

4.4.2. The effects of graphene-based nanomaterials on lysosome in cancer cells

It was recently found that the graphene nanosheets (362.3 nm) are mainly distributed in the lysosomes [105]. The integrity of lysosome can be disrupted thereby permeabilize lysosomal membrane and cause cell death. Graphene nanosheets could cause physical damage to plasma membrane and organelle membranes such as lysosome (increased lysosomal membrane permeability) and mitochondria (depolarized the mitochondrial membrane potential) through the physical interaction and excessive production of ROS in rat basophilic leukemia (RBL-2H3) cells [105].

Photodamage in lysosomes could be induced to destroy the cancer cells. rGO loaded with PEG-modified Ru (II) complex (Ru-PEG) (thickness of 25 nm) was used for lysosome-targeted phosphorescent imaging and combined photothermal therapeutic (PTT)-photodynamic therapeutic (PDT) therapy. The Ru-PEG could be released from rGO in the acidic solution (pH 5) mimicking the lysosomal/endosomal environments, that can be correlated with the protonation/deprotonation process of carboxyl groups on rGO. Under light excitation, apoptosis is induced by rGO-Ru-PEG through ROS generation and cathepsin-initiated apoptotic signaling pathway (Fig. 4B) [106]. Therefore, besides the physical damages of lysosome in cancer cells by graphene, we could also benefit from the pH-dependent drug release property of GO-based nanohybrids in lysosomes, that is an effective strategy for the multifunctional imaging and phototherapy of cancer.

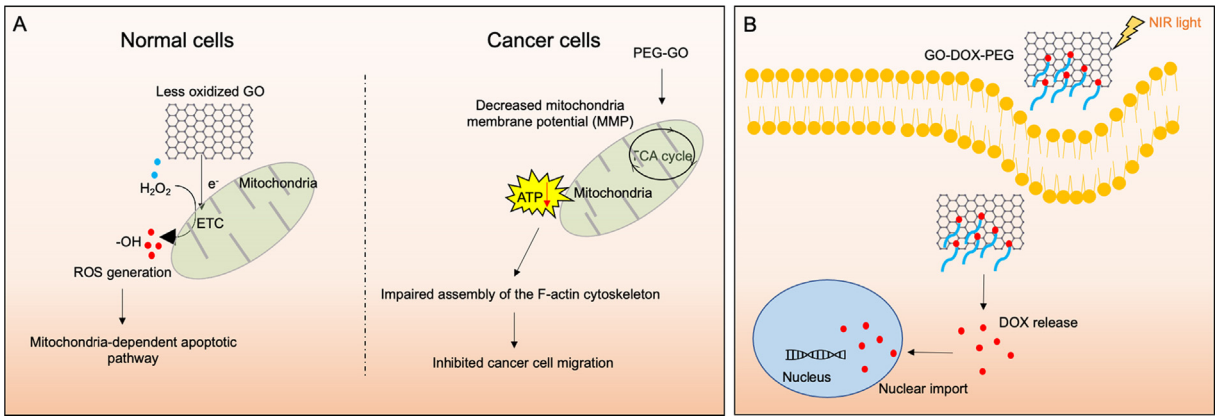

Fig. 5. The mechanism of GO functions in A) mitochondria of normal and cancerous cells and B) nucleus of cancerous cells. A) GO acts as an electron donor and accelerates the ROS generation followed by mitochondria-dependent apoptotic pathway [108]. PEG-GO leads to the impairment of ATP production and inhibited cancer cell migration [11]. B) Drug is released from GO-DOX-PEG and translocated to nucleus [114].

4.4.3. The effects of graphene-based nanomaterials on mitochondria in normal cells

GO and GO-related nanomaterials can interact with the mitochondria, modulate their morphology and function, and decrease the mitochondrial membrane potential (MMP) [32]. It was found that the pristine graphene (500–1000 nm) induced mitochondrial depolarization in macrophages is associated with mitochondrial dysfunction and overproduction of ROS. It is followed by the activation of mitochondria-dependent apoptotic pathway through redistributing mitochondrial cytochrome *c* and caspases activation, which ultimately resulted in cell death [107].

Pristine graphene (500–1000 nm at range of 5–20 μg/mL) induced the generation of intracellular ROS in a concentration and time-dependent manner [51]. GO material acting as an electron donor, supplies electrons to complexes I and II of the ETC and accelerates the ROS generation as the byproduct of mitochondrial respiration. However, the production of ROS by electron donation depends on the chemical characteristics (oxidation degree) of graphene nanomaterials. As less oxidized GO particles (200–260 nm) produced higher levels of ROS due to the fact that they have more free electrons, stronger oxidative ability, higher facilitative ability on production of ·OH radical from H_2O_2, and electron transfer during the reactions (Fig. 5A). Furthermore, carboxyl groups on the GO lowering the energy barrier of H_2O_2 decomposition, facilitates the reaction process [108].

Therefore, given the oxidation degree-dependent ROS generation by GO, we would suggest optimizing the oxidation degree of GO to lower ROS production and ensure the biocompatibility in normal cells. This conclusion is consistent with previous report on the biocompatibility of oxidized graphene nanoplatelets (1:6) in human fibroblasts [77].

4.4.4. The effects of graphene-based nanomaterials on mitochondria in cancer cells

GO is internalized and mainly entrapped within lysosome, while a small proportion of graphene relocated to the cytosol and interacted with the mitochondria [9,10,96]. Degradation of mitochondria and oxidative stress are considered as the main mechanism of toxicity of graphene platelets with irregular and sharp edges (4 μm) on both U87 glioblastoma cells and tumors and HS-5 non-cancer cells [109]. Perturbation of the mitochondrial structure and function was shown in the human hepatoma cell line exposed to $\geq$ 8 μg/mL of GO (385 nm) by a decrease in MMP and dysregulation of mitochondrial Ca^{2+} homeostasis [69,107]. The same cell line treated with 40 nm sized GO (EC20 10 mg/L and EC50 81 mg/L)/rGO (EC20 8 mg/L and EC50 46 mg/L). The results showed a marked dose- and time- dependent depolarization in MMP for 4 h and 24 h [62].

PEG functionalization of GO enhances the biocompatibility and stability of GO. PEG-modified GO (PEG-GO) (100–200 nm) up to 80 μg/mL concentration exhibited no apparent effect on the viability of breast cancer or non-cancerous cells. However, exposing breast cancer cells to PEG-GO (40 μg/mL) differentially up- and down-regulated various biological pathways in breast cancer versus normal cells while no toxicity was still observed for normal cells under same experimental condition. PEG-GO inhibited the migratory and invasive properties of human metastatic breast cancer cell lines by down-regulating the expression of genes involved in energy metabolism, inhibition of ETC complexes I, II, III, and IV, resulting in mitochondria depolarization and impairment of ATP production. It leads to a disruption of F-actin cytoskeletal assembly that in turn impaired cell migration as the treatment for metastasis in breast cancer [11] (Fig. 5A). Thus, the PEG-modification of GO improved its aqueous stability and biocompatibility, enhancing its potential for treating metastatic breast cancer. Based on this finding and potential mitochondria targeting of PEG-GO in cancer cells, the PEG-GO-based nanostructures were used for the delivery of xanthohumol, a potent inhibitor of electron transfer chain (ETC) complex I, for the metastasis therapy *in vivo* [110].

Beside mitochondria function in cellular energy balance, metabolism, modulation of calcium signaling, and cellular redox balance, it also plays a crucial role in the induction of cell death by rGO [107,111,112]. As the rGO with 200 nm size (at IC50 concentration: 15.12 μg/mL) inhibited the proliferation of human breast cancer cells, leading to programmed cell death and activation of mitochondrial-mediated signaling pathway with the involvement of the NF-κB signaling pathway [111]. This is consistent with the effect of rGO surface chemistry on the involvement of toll-like receptor (TLR4-NF-κB) signaling pathway [62].

Considering ROS generation as the byproduct of mitochondrial respiration, GO (385 nm) at range of 1–16 μg/mL could also induce generation of intracellular ROS in a concentration and time-dependent manner in the human hepatoma cell line [69,107]. ROS generation is also introduced by GO after near-infrared (NIR) irradiation in mice. GO (~100 nm) can sensitize the formation of intracellular ROS such as singlet oxygen to exert combined nanomaterial-mediated PDT and PTT effects on the destruction of mice melanoma tumors using ultra-low doses of NIR light (~0.36 W/cm^2) [113]. After NIR irradiation, GO-DOX-PEG nanodrug (149 nm) (5 μg/mL DOX equivalent concentration) also increased higher levels of intracellular ROS compared to GO-DOX and free DOX [114]. ROS generation was also proved the potential applicability of GO-ZnO nanocomposites (62 nm) in treatment of breast cancer cells [115]. Thus, ROS generation induced by GO in cancerous cells is found as a useful strategy for cancer therapy. Several factors including size, shape, surface area, surface charges, surface-associated chemical groups, solubility and dispersion, ions released from graphene, photo-activation, aggregation, mode of interaction with cells, the presence of inflammation in tissues, and pH determine the graphene-induced toxicity by ROS generation [116].

Moreover, a GO-based two-step targeting system was designed to target first tumor and then mitochondria. GO was modified with integrin αvβ3 monoclonal antibody (mAb) to bind the antigens on tumor cells. Pyropheophorbide a (PPa) was conjugated with PEG to cover the GO surface and gain phototoxicity. This system effectively targets the αvβ3-positive tumor cells with 80 % accumulation at mitochondria during 8 h post treatment [9]. The mitochondria targeting and phototoxicity of this system shows the potential of GO as an efficient photosensitizer carrier that increases the efficiency of PDT.

Glycyrrhetinic acid (GA) is known as the mitochondria targeting ligand and it basically could improve the drug uptake through enhanced permeability of mitochondria. Thus, GA-functionalized GO was applied for the targeted delivery of doxorubicin into mitochondria and it significantly induced apoptosis through the mitochondria-mediated apoptosis [117].

Altogether, perturbation of the mitochondrial structure and function, membrane potential depolarization, impaired ATP production, ROS generation could be suggested as the outcomes from the interaction of GO nanomaterials with mitochondria in cancer cells, that can be applied for cancer therapy and metastasis treatment.

4.4.5. The effects of graphene-based nanomaterials on nucleus in cancer cells

There is no specific information on the interaction of GO nanomaterials with nucleus in normal cells, then we have only included the information on the interaction of GO nanomaterials with cancer cells.

GO (51 nm) could localize in cytosol, mitochondria, endoplasmic reticulum (ER), and nucleus. Translocated GO from the cytosol into the nucleus can be passed through nuclear pore complexes

(NPCs) with a central channel up to 40 nm of particle size, hence nanomaterial size should be adjusted to<40 nm for nuclear transport [96]. GO (300 nm) at 100 and 300 μg/mL concentrations entered to A549 human lung adenocarcinoma cells and without causing any cell damage located in the cytoplasm and nucleus after 4 h [118]. However, mechanism of GO transfer to nucleus was not shown and further evidence is needed to support this hypothesis. Similarly, Zuchowska et al., (2020) showed high affinity of GO flakes to nucleus in cancer cells, that affect the metabolism and inhibits proliferation in cancer cells [119]. GQDs also specifically interact with DNA and they can be considered as the naturally nucleus-targeting anticancer reagent [120]. Thus, nucleus targeted tumor therapy can be developed through DNA damage using GQDs.

Chemotherapy drugs are delivered to the nucleus using graphene nanomaterials as the nanocarrier. DOX was efficiently delivered to the nucleus by GQDs (~30 nm). Increased DOX nuclear uptake enhanced the cytotoxicity of DOX in drug-resistant cancer cells [121]. Furthermore, the NIR and pH dual-responsive GO-DOX-PEG nanodrug (about 140 nm) was developed by noncovalent modification. Conjugating PEG with GO weakened the bond between DOX-PEG and GO, resulting in a better drug release, nuclear translocation of nanodrugs and thereby improved the treatment effect [114] (Fig. 5B).

In another approach, the cytotoxicity of combined application of GO with cisplatin were evaluated against colon, ovarian, cervical, and prostate cancer cells. The mechanism of effect was through triggering the acetylation of histone H4 in the nucleus, hence the chromosome could be decondensed and cisplatin could approach chromosomal DNA and trigger cell death [122]. In another example, 50 mg/mL of GO (450 nm) combined with 200 mg/mL *cis*-diaminedichloroplatinum (CDDP) potentiated killing CT26 colon cancer cells via necrosis. It could lead to autophagy marker LC3 trafficking towards the nucleus in an importin-α/β-dependent manner, that coincided with the CDDP nuclear import and necrosis [123]. Therefore, GO itself can be used together with anticancer drugs, chemosensitize the cancer cells to drug, and enhance the efficacy of therapy.

Overall, GO at small size and GQD could be translocated to the nucleus and interact with DNA in cancer cells, that is beneficial for inhibition of proliferation in cancer cells.

4.4.6. The effects of graphene-based nanomaterials on ER in normal and cancer cells

Unfunctionalized few-layer graphene (FLG) (265 nm) is graphene materials and formulations with not or low defects in the sheet structure. No significant effect on viability of macrophages was observed by low doses exposure to FLG however, it elicited a significant oxidative stress leading to autophagy via ER stress [124].This is consistent with ER stress induced by GO-PEG (1.1 × 5 00 nm) in vaginal epithelial cells [125].

When it comes to cancer cells, GO (51 nm) could localize in ER [96] and even ER was less visible in glioblastoma cells after treatment with both GO- (100 nm to 10 μm) and rGO (100 nm to 1.5 μm) [126]. High rate of proliferation in cancer cells and increased protein demands could lead to ER stress with accumulation of misfolded and/or unfolded proteins in the ER lumen. Thus, ER-targeted self-assembled graphene oxide nanoparticles encompassing ER stress inducers, (doxorubicin and cisplatin) were designed that efficiently prompting ER stress associated apoptosis in lung, breast, and drug resistant breast cancer cells [127].

Overall, the ER targeting can be proposed as a useful strategy exploiting ER stress as a target leading to better cancer therapeutics.

4.4.7. The effects of graphene-based nanomaterials on peroxisome in normal and cancer cells

Based on the current knowledge, there is no report on direct physical interaction between GO nanomaterials and peroxisome. However, exposure to large size GO (500–5000 nm) but not small size GO (<500 nm) reduced lipid accumulation in macrophages [128]. It also negatively affects the protein and mRNA levels of key components in peroxisome proliferators-activated receptor (PPAR) signaling pathway that is related to the lipid droplet biogenesis.

Lipid droplets act as the lipid storage for energy generation, membrane synthesis, and protein degradation [129]. The diminished levels of intracellular lipids after treatment with gambogic acid and graphene revealed that graphene delivery improved the cytotoxic effects of gambogic acid in breast and pancreatic cancer cells [130].

Thus, given the size effect of GO nanomaterials on lipid accumulation by peroxisome in normal cells, we would need tailoring the size in a way that not reducing the lipid accumulation for supplying enough energy and ensuring membrane integrity.

4.5. Dose-dependent effects of graphene-based nanomaterials in normal and cancer cells

There are plenty of reports showing the dose-dependent toxicity of GO. GO at concentration of < 20 μg/mL was observed to be nontoxic to human fibroblast cells, but at concentration > 50 μg/mL caused cytotoxicity by inducing cell apoptosis [131].

The dose-dependent interaction of graphene nanoplatelets with cells depends on the size and sharpness of particle edges. Large graphene nanoplatelets (5 μm) with the sharp and long edges caused membrane damages and they are cytotoxic to human fibroblasts above 20 μg/mL. The smaller nanoplatelets (1–2 μm) internalized without membrane damages. They enhanced ROS generation and are toxic to human fibroblasts above 50 μg/mL. Thus, the smaller nanoplatelets (1–2 μm) are more biocompatible and they cause cytotoxicity at higher concentration (above 50 μg/mL) [77]. Interestingly, sharp edges in large graphene nanoplatelets folded by complete oxidation reaching the oxygen content of 24 % (mostly carboxyls and hydroxyls) and thereby assuring the biocompatibility until the highest concentration (100 μg/mL) [77]. It is consistent with the higher oxidation degree of GO that is coupled with lower ROS generation and higher biocompatibility [108].

In case of cancerous cells, the exposure of 16 μg/mL GO platelets (383 nm) for 24 h completely covered the surface of liver cancer cells, while 8 μg/mL (314 nm) and lower concentrations only covered part of the cell surface [69]. It was shown that in the absence of cell death, GO triggered membrane ruffling in a variety of different cell lines [132,133].

There are several examples of heterogenous cell-specific GO cytotoxicity. GO at lower concentrations (1–10 μg/mL) was shown to be least toxic to MCF-7 cancer cells [134]. But even at very low concentrations (8 μg/mL), GO changes the cellular metabolism in HepG2 carcinoma cells [69].

Hence, the dose-dependent interaction of GO is significantly differed with respect to different cell lines. It can be due to differences in uptake process among different cell lines. As majority of GO can be taken up by some cell types through phagocytosis while in some other types of cells, GO can be only internalized through clathrin-mediated endocytosis with size limit, that limits the number of GOs with internalization capacity.

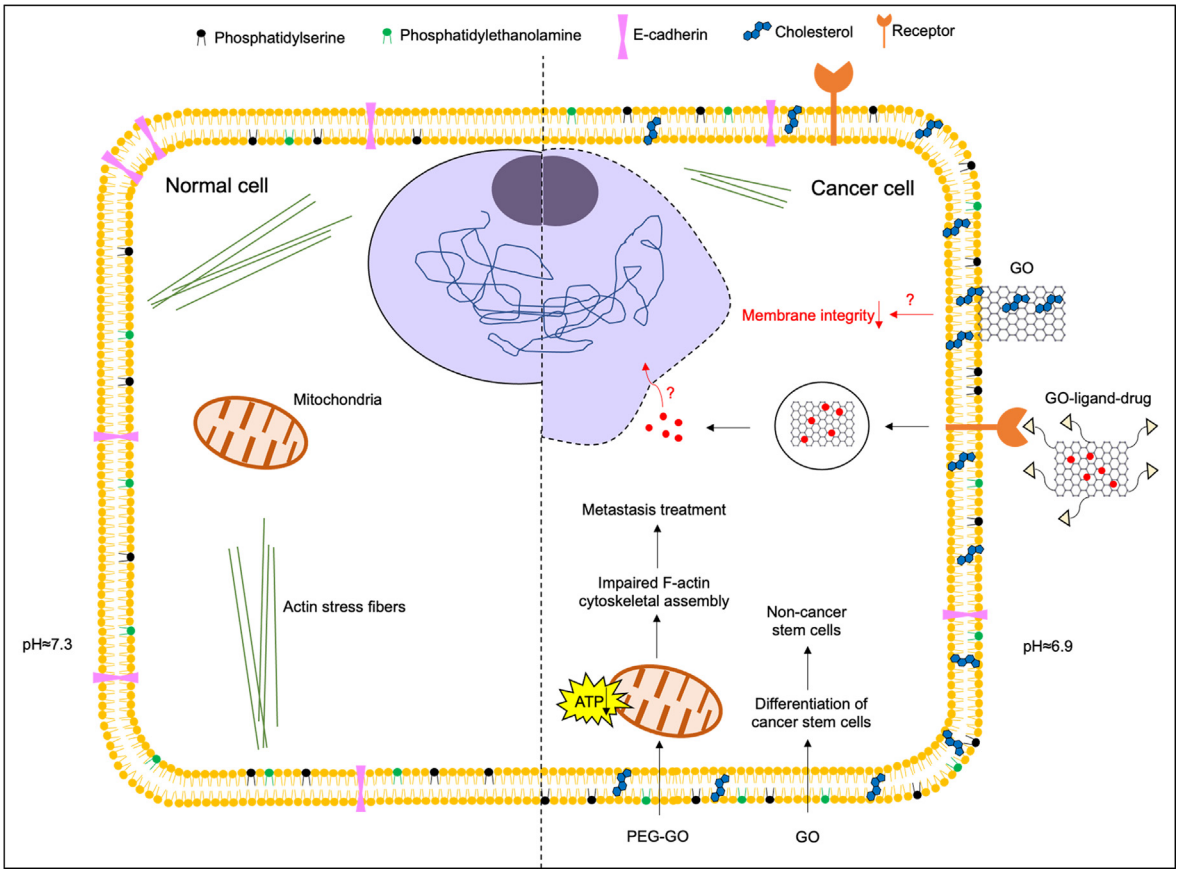

Fig. 6. The applications of GO interaction with cancer cells for cancer therapy. Polyethylene glycol (PEG)-modification of GO can be used as a potential treatment for metastasis. Promoting the differentiation of cancer stem cells into non-cancer stem cells using GO is an effective therapeutic strategy. GO conjugated with targeting ligand bind to receptor on the tumor cell surface followed by receptor-mediated endocytosis and thereby improving the accuracy of the anti-tumor drug delivery to the target sites. Abnormally perforated nucleus envelop in cancerous cells might cause drug itself or in conjugation with GO translocated to the nucleus. Graphene might extract cholesterol that are in higher numbers on the membrane of multidrug resistant cells, leading loss of membrane integrity and cytotoxicity.

5. Applications of graphene-based nanomaterials in cancer therapy

5.1. Application of graphene-based nanomaterials for metastasis therapy

Based on our elucidations in previous sections, the interaction of GO nanomaterials with cytoskeleton could be utilized for metastasis treatment. However, GO could also disrupt cytoskeleton assembly in normal cells. But treatment with PEG-modified GO showed minimal toxicity to normal cells while it impaired ATP production by mitochondria, disrupted F-actin cytoskeletal assembly, and impaired cell migration in cancer cells. Thus, PEG-GO itself or as the mitochondria targeted drug delivery could be a potential treatment for metastasis [11,110] (Fig. 6). It is notable that PEG-GO with different sizes from nanosize (100–200 nm) to microsize (1–5 μm) had no or negligible effect on the cell viability and we could ignore the particle size effect on cytotoxicity [41].

Some other methods such as covering the cancer cell surface by GO and blocking the interaction of membrane proteins and external ligands and their downstream pathways could also beneficially inhibit metastasis [98].

Disruption of the extracellular matrix (ECM) in liver can deregulate the interaction of ECM-cell, and lead to uncontrolled proliferation. While an artificial ECM with mechanical and physicochemical properties of healthy tissue can reduce invasiveness of cancer cells. For example, HepG2 cancer cells could grow on mimic ECM, a GO nanofilm that is in interaction with a natural protein cocktail derived from liver of chicken embryo. In this way, we could reduce the uncontrolled proliferation of tumor cells through adhesion, integrin expression, morphology change, and cell cycle arrest in the G2/M phase [135].

Overall, we described several potential methods that GO can beneficially interact with the cells for metastasis therapy.

5.2. Application of graphene-based nanomaterials as the drug carrier for cancer therapy

For drug delivery application of GO nanomaterials, we would need to consider the GO interaction with biomolecules like proteins, and tailoring the number of layers (MLGO), oxidation degree, and functionalization (PEG, polyacrylic acid (PAA), and D-mannose). It ensures invisibility of carrier to the immune system leading longer systemic circulation and higher rate of drug delivery to the target sites. Furthermore, functionalization could also eliminate the particle size effect on internalization process and thereby ensure reduced cytotoxicity and improved biocompatibility in normal cells.

As the fundamental differences between cancer and normal cells, higher expression of specific receptors on the surface of cancerous cells could be exploited for graphene-based targeted drug delivery. GO nanocarriers conjugated with different targeting ligands bind to cancer specific receptors on the tumor cell surface followed by receptor-mediated endocytosis and thereby improving the accuracy of the anti-tumor drug delivery to the target sites. Folate receptor, CD44, gastrin-releasing peptide (GRP) receptor, formyl peptide receptor, dopamine receptor, transferrin and death receptor are examples of some receptors used in graphene-based receptor-mediated targeted drug delivery [136–148].

Therefore, the proper interaction of functionalized GO with the biomolecules and receptors on the cell surface could make the GO nanomaterials into a promising biocompatible and targeted drug delivery system for cancer therapy.

5.3. Application of graphene-based materials effects on cancer stem cell differentiation for cancer therapy

Cancer stem cells (CSCs), a subpopulation of tumor cells, show resistance to the conventional chemotherapy. They self-renew, differentiate, and form new type of tumor cells or even transdifferentiate into normal non-cancer cells, such as vascular endothelial cells and pericytes [149]. These cells differentiate to form a small mass of cells known as a tumor-sphere. Interestingly, GO flakes with two distinct sizes ranging from 0.2 to 2 μm and from 5 to 20 μm prevented the cells to form tumor-sphere in multiple cell lines (breast, ovarian, prostate, lung and pancreatic cancers, and glioblastoma (brain)). GO forced the cancerous cells to differentiate into non-cancer stem-cells through inhibition of signaling pathways involved in CSC self-renewal including wingless-int (Wnt), notch, and signal transducer and activator of transcription (STAT) [150].

Furthermore, GO combined with silver nanoparticles (GO-AgNPs) was used to treat SH-SY5Y neuroblastoma CSCs. GO-AgNP caused ROS-dependent neuronal differentiation. It increased expression of Akt, ERK1/2, P53, or *P*21 signaling pathways that are involved in cell cycle control and cell differentiation in the neuroblastoma cells [151].

Therefore, promoting the differentiation of CSC using GO could be an effective therapeutic strategy for cancer [149,152].

6. Challenges and future directions

Despite potential application of GO for metastasis treatment, cytotoxic interactions of GO with mitochondria (mitochondrial depolarization, overproduction of ROS, the activation of mitochondria-dependent apoptotic pathway through redistributing mitochondrial cytochrome *c*, caspases activation and cell death) and cytoskeleton (regulation of cytoskeleton-associated genes as well as alterations in cell cycle and cell death) in non-cancerous cells limit the applications of GO. However, proper functionalization of GO for example with PEG would be necessary to help reducing the side effects of GO on non-cancerous cells. Furthermore, more efforts are also required towards the functionalization-driven biocompatibility to provide extensive evidence about the biosafety of GO in different cell lines, *in vivo* and long-term toxicity assessment.

It is well-documented that the GO nanomaterials affect the cytoskeleton assembly in both normal and cancer cells. However, considering less dense and less organized actin stress fibers in cancer cells as the fundamental difference compared to normal cells, we might suppose to have more pronounced cytotoxicity of GO nanomaterials against cancer cells compared to normal cells, that is not yet studied.

Notwithstanding inherent advantages of GO as a delivery platform, it needs to be surface engineered to develop targeted drug delivery systems, providing specific toxic interaction with cancerous cells and limiting their toxicity to normal cells. Furthermore, considering the effect of size and oxidation degree of GO on interaction with plasma membrane and internalization, the engineering of size and oxidation degree of GO nanomaterials would be needed to ensure proper internalization through endocytosis while minimizing harm to the plasma membrane.

Given the abnormally deformed and perforated nucleus envelop in cancerous cells as their structural difference compared to normal cells, we might assume that drug itself or conjugated with GO translocated to the nucleus in larger quantity compared to normal cells leading more cytotoxic interaction with nucleus in cancer cells, that is not yet investigated (Fig. 6).

Given the altered cholesterol metabolism and increased cholesterol level in multi-drug resistant cancer cell membrane as explained before, we would presume that graphene materials interact differently with these cells compared to normal cells. In fact, the graphene might extract cholesterol that are in higher numbers on the membrane of multidrug resistant cells, leading loss of membrane integrity and cytotoxicity, that needs to be proved (Fig. 6).

There are several novel compounds such as half-sandwich Ru complexes with significant selectivity towards cancer cells (mitochondrial dysfunction, ROS production, and lysosomal destruction) over normal cells [153]. Such selective class of complexes are a good example of cargo for graphene-based delivery platforms with fewer side effects.

It has been shown that GO pretreatment or combined treatment with classic anticancer drugs can improve the treatment efficacy by sensitizing cancer cells to chemotherapeutic agents. However, this strategy needs to be focalized to only cancer cells to avoid unwanted effects of GO to non-cancerous cells, and further information about the GO biodistribution and clearance from the body need to be generated.

The persistence of GO nanomaterials in the body is one of the big challenges for the application of GO in the clinic. One venue would be to investigate the ability of the human body (e.g. using human lung myeloperoxidase (MPO), or other biological systems such as e.g. commensal bacteria, to degrade these nanomaterials. An alternative venue would be to further functionalize GO in such a way that its clearance from the body would be increased. Designing biodegradable or high-clearance tailored GO conjugates would be an important steppingstone towards real therapeutic applications.

7. Conclusion

From the interaction studies of GO with cancerous cells, the potential applications of GO features can be exploited for i) metastasis therapy through cytotoxic interaction of GO with mitochondria and F-actin cytoskeleton assembly in cancerous cells, ii) lysosome-targeted photodamage in cancer cells through cytotoxic interaction of GO with lysosome, iii) sensitizing cancer cells to chemotherapeutic agents by compromising plasma membrane and cytoskeleton meshwork, and iv) differentiation of cancer stem cells into non-cancer stem-cells (Box 1, Fig. 6).

Box 1 Applications of GO features for cancer therapies.

1. Engineering number of layers, oxidation degree, and functionalization of GO is needed for invisibility of GO to the immune system.
2. Engineering GO surface chemistry into hydrophilic/hydrophobic ensures the internalization process through endocytosis/membrane adsorption.
3. Proper functionalization of GO limits the cytotoxicity of particle size effect.
4. PEG-modification of GO is a potential treatment for metastasis through the cytotoxic interactions with cytoskeleton and mitochondria.
5. GO conjugated with ligands for receptors on the cancer cell surface ensures receptor-mediated targeted drug delivery to the cancer cells.
6. Promoting the differentiation of cancer stem cells (CSC) into non-cancer stem-cells using GO is an effective therapeutic strategy.
7. GO pretreatment compromising plasma membrane and cytoskeleton meshwork sensitizes cancer cells to chemotherapeutic agents and improves the treatment efficacy.

The interaction studies of GO with non-cancerous cells suggest that some critical parameters for fabrication of stable and biocompatible GO need to be considered (Box 2). Well-engineered GO with appropriate size, side length, oxidation degree, surface functional groups, and functionalization could assure the biocompatibility and reduced cytotoxicity against normal cells.

Box 2 Critical parameters need to be considered for fabrication of biocompatible GO.

- Size- GO with<100 nm shows highest cytotoxicity even at low concentration (5 mg/L). Medium sized GO (300 nm) is more biocompatible. Microsized GO (1–3 μm) at high dose (100 mg/L) and long exposure causes physical damages.
- Side length- Oxidized graphene with side length 3.5 nm adsorbs graphene on the membrane surface and less oxidized graphene with 10.5 nm side length can be used for graphene internalization through endocytosis.
- Oxidation degree- Graphene nanoplatelets oxidized with ratio 1:6 even at high concentrations assuring biocompatibility lasting up to 72h.
- Surface functional groups- Carbon radicals determine following biocompatibility for GO nanomaterials; reduced GO (rGO)> pristine GO> hydrated GO (hGO)
- Functionalization- Proper functionalization with poly (acrylic acid) (PAA) and polyethylene glycol (PEG) could make GO invisible to immune system, change the corona protein formation, and enhance the circulation time.

From the *in vitro* and *in vivo* studies reviewed here; it can be concluded that the graphene-based nanoplatform is a promising material for cancer therapy with various applications from metastasis treatment to drug carrier, and non-cancer stem cell differentiation.

Data availability

No data was used for the research described in the article.

Declaration of Competing Interest

The authors declare that they have no known competing financial interests or personal relationships that could have appeared to influence the work reported in this paper.

Acknowledgment

This study was supported by a grant from the Vinnova – Sveriges innovationsmyndighet [2020-00792], a grant from the Novo Nordisk Foundation [NNF20OC0064547], and a grant from Kristina Stenborgs foundation for scientific research [C 2021-1705].

References

[1] F. Bray, J. Ferlay, I. Soerjomataram, R.L. Siegel, L.A. Torre, A. Jemal, Global cancer statistics 2018: GLOBOCAN estimates of incidence and mortality worldwide for 36 cancers in 185 countries, CA. Cancer J. Clin. 68 (2018) 394–424. https://doi.org/10.3322/caac.21492.

[2] Z. Tu, G. Guday, M. Adeli, R. Haag, Multivalent Interactions between 2D Nanomaterials and Biointerfaces, Adv. Mater. 30 (2018) 1706709, https://doi.org/10.1002/adma.201706709.

[3] Y. Qu, F. He, C. Yu, X. Liang, D. Liang, L. Ma, Q. Zhang, J. Lv, J. Wu, Advances on graphene-based nanomaterials for biomedical applications, Mater. Sci. Eng. C. 90 (2018) 764–780, https://doi.org/10.1016/j.msec.2018.05.018.

[4] P. Wick, A.E. Louw-Gaume, M. Kucki, H.F. Krug, K. Kostarelos, B. Fadeel, K.A. Dawson, A. Salvati, E. Vázquez, L. Ballerini, M. Tretiach, F. Benfenati, E. Flahaut, L. Gauthier, M. Prato, A. Bianco, Classification Framework for Graphene-Based Materials, Angew. Chemie Int. Ed. 53 (2014) 7714–7718, https://doi.org/10.1002/anie.201403335.

[5] M. Orecchioni, R. Cabizza, A. Bianco, L.G. Delogu, Graphene as Cancer Theranostic Tool: Progress and Future Challenges, Theranostics. 5 (2015) 710–723, https://doi.org/10.7150/thno.11387.

[6] O.N. Ruiz, K.A.S. Fernando, B. Wang, N.A. Brown, P.G. Luo, N.D. McNamara, M. Vangsness, Y.-P. Sun, C.E. Bunker, Graphene Oxide: A Nonspecific Enhancer of Cellular Growth, ACS Nano. 5 (2011) 8100–8107, https://doi.org/10.1021/nn202699t.

[7] C. Zhao, S. Pandit, Y. Fu, I. Mijakovic, A. Jesorka, J. Liu, Graphene oxide based coatings on nitinol for biomedical implant applications: effectively promote mammalian cell growth but kill bacteria, RSC Adv. 6 (2016) 38124–38134, https://doi.org/10.1039/C6RA06026A.

[8] F. Bani, M. Adeli, S. Movahedi, M. Sadeghizadeh, Graphene-polyglycerol-curcumin hybrid as a near-infrared (NIR) laser stimuli-responsive system for chemo-photothermal cancer therapy, RSC Adv. 6 (2016) 61141–61149, https://doi.org/10.1039/c6ra05917a.

[9] Y. Wei, F. Zhou, D. Zhang, Q. Chen, D. Xing, A graphene oxide based smart drug delivery system for tumor mitochondria-targeting photodynamic therapy, Nanoscale. 8 (2016) 3530–3538, https://doi.org/10.1039/C5NR07785K.

[10] H. Zhou, B. Zhang, J. Zheng, M. Yu, T. Zhou, K. Zhao, Y. Jia, X. Gao, C. Chen, T. Wei, The inhibition of migration and invasion of cancer cells by graphene via the impairment of mitochondrial respiration, Biomaterials. 35 (2014) 1597–1607, https://doi.org/10.1016/j.biomaterials.2013.11.020.

[11] T. Zhou, B. Zhang, P. Wei, Y. Du, H. Zhou, M. Yu, L. Yan, W. Zhang, G. Nie, C. Chen, Y. Tu, T. Wei, Energy metabolism analysis reveals the mechanism of inhibition of breast cancer cell metastasis by PEG-modified graphene oxide nanosheets, Biomaterials. 35 (2014) 9833–9843, https://doi.org/10.1016/j.biomaterials.2014.08.033.

[12] Q. Zhang, Z. Wu, N. Li, Y. Pu, B. Wang, T. Zhang, J. Tao, Advanced review of graphene-based nanomaterials in drug delivery systems: Synthesis, modification, toxicity and application, Mater. Sci. Eng. C. 77 (2017) 1363–1375, https://doi.org/10.1016/j.msec.2017.03.196.

[13] J. Liu, J. Dong, T. Zhang, Q. Peng, Graphene-based nanomaterials and their potentials in advanced drug delivery and cancer therapy, J. Control. Release. 286 (2018) 64–73, https://doi.org/10.1016/j.jconrel.2018.07.034.

[14] K. Yang, Y. Li, X. Tan, R. Peng, Z. Liu, Behavior and toxicity of graphene and its functionalized derivatives in biological systems, Small. 9 (2013) 1492–1503, https://doi.org/10.1002/smll.201201417.

[15] X. Hu, Q. Zhou, Health and ecosystem risks of graphene, Chem. Rev. 113 (2013) 3815–3835, https://doi.org/10.1021/cr300045n.

[16] C. Jiang, H. Zhao, H. Xiao, Y. Wang, L. Liu, H. Chen, C. Shen, H. Zhu, Q. Liu, Recent advances in graphene-family nanomaterials for effective drug delivery and phototherapy, Expert Opin. Drug Deliv. 18 (2021) 119–138, https://doi.org/10.1080/17425247.2020.1798400.

[17] S.K. Singh, M.K. Singh, P.P. Kulkarni, V.K. Sonkar, J.J.A. Grácio, D. Dash, Amine-Modified Graphene: Thrombo-Protective Safer Alternative to Graphene Oxide for Biomedical Applications, ACS Nano. 6 (2012) 2731–2740, https://doi.org/10.1021/nn300172t.

[18] G. Perini, V. Palmieri, G. Ciasca, M. D'ascenzo, J. Gervasoni, A. Primiano, M. Rinaldi, D. Fioretti, C. Prampolini, F. Tiberio, W. Lattanzi, O. Parolini, M. De Spirito, M. Papi, Graphene quantum dots' surface chemistry modulates the sensitivity of glioblastoma cells to chemotherapeutics, Int. J. Mol. Sci. 21 (2020) 1–17, https://doi.org/10.3390/ijms21176301.

[19] M. Orecchioni, L. Fusco, R. Mall, V. Bordoni, C. Fuoco, D. Rinchai, S. Guo, R. Sainz, M. Zoccheddu, C. Gurcan, A. Yilmazer, B. Zavan, C. Ménard-Moyon, A. Bianco, W. Hendrickx, D. Bedognetti, L.G. Delogu, Graphene oxide activates B cells with upregulation of granzyme B expression: evidence at the single-cell level for its immune-modulatory properties and anticancer activity, Nanoscale. 14 (2022) 333–349, https://doi.org/10.1039/D1NR04355B.

[20] M. Georgieva, B. Vasileva, G. Speranza, D. Wang, K. Stoyanov, M. Draganova-Filipova, P. Zagorchev, V. Sarafian, G. Miloshev, N. Krasteva, Amination of Graphene Oxide Leads to Increased Cytotoxicity in Hepatocellular Carcinoma Cells, Int. J. Mol. Sci. 21 (2020) 2427, https://doi.org/10.3390/ijms21072427.

[21] P. Makvandi, M. Ghomi, M. Ashrafizadeh, A. Tafazoli, T. Agarwal, M. Delfi, J. Akhtari, E.N. Zare, V.V.T. Padil, A. Zarrabi, N. Pourreza, W. Miltyk, T.K. Maiti, A review on advances in graphene-derivative/polysaccharide bionanocomposites: Therapeutics, pharmacogenomics and toxicity, Carbohydr. Polym. 250 (2020), https://doi.org/10.1016/j.carbpol.2020.116952 116952.

[22] M. Sattari, M. Fathi, M. Daei, H. Erfan-Niya, J. Barar, A.A. Entezami, Thermoresponsive graphene oxide – Starch micro/nanohydrogel composite as biocompatible drug delivery system, BioImpacts. 7 (2017) 167–175, https://doi.org/10.15171/bi.2017.20.

[23] A. Deb, R. Vimala, Natural and synthetic polymer for graphene oxide mediated anticancer drug delivery—A comparative study, Int. J. Biol. Macromol. 107 (2018) 2320–2333, https://doi.org/10.1016/j.ijbiomac.2017.10.119.

[24] M. Xie, F. Zhang, H. Peng, Y. Zhang, Y. Li, Y. Xu, J. Xie, Layer-by-layer modification of magnetic graphene oxide by chitosan and sodium alginate with enhanced dispersibility for targeted drug delivery and photothermal therapy, Colloids Surfaces B Biointerfaces. 176 (2019) 462–470, https://doi.org/10.1016/j.colsurfb.2019.01.028.

[25] G.R. Bardajee, Z. Hooshyar, A novel thermo-sensitive nanogel composing of poly(N-isopropylacrylamide) grafted onto alginate-modified graphene oxide

for hydrophilic anticancer drug delivery, J. Iran. Chem. Soc. 15 (2018) 121–129, https://doi.org/10.1007/s13738-017-1215-9.
[26] M. Xie, F. Zhang, L. Liu, Y. Zhang, Y. Li, H. Li, J. Xie, Surface modification of graphene oxide nanosheets by protamine sulfate/sodium alginate for anti-cancer drug delivery application, Appl. Surf. Sci. 440 (2018) 853–860, https://doi.org/10.1016/j.apsusc.2018.01.175.
[27] Z. Rao, H. Ge, L. Liu, C. Zhu, L. Min, M. Liu, L. Fan, D. Li, Carboxymethyl cellulose modified graphene oxide as pH-sensitive drug delivery system, Int. J. Biol. Macromol. 107 (2018) 1184–1192, https://doi.org/10.1016/j.ijbiomac.2017.09.096.
[28] O.P. Troncoso, F.G. Torres, Bacterial Cellulose — Graphene Based Nanocomposites (2020) 1–17.
[29] S. Kim, M.J. Moon, S.P. Surendran, Y.Y. Jeong, Biomedical applications of hyaluronic acid-based nanomaterials in hyperthermic cancer therapy, Pharmaceutics. 11 (2019) 1–19, https://doi.org/10.3390/pharmaceutics11070306.
[30] R. Lima-Sousa, D. de Melo-Diogo, C.G. Alves, E.C. Costa, P. Ferreira, R.O. Louro, I.J. Correia, Hyaluronic acid functionalized green reduced graphene oxide for targeted cancer photothermal therapy, Carbohydr. Polym. 200 (2018) 93–99, https://doi.org/10.1016/j.carbpol.2018.07.066.
[31] S.Y. Lee, M.S. Kang, W.Y. Jeong, D.W. Han, K.S. Kim, Hyaluronic acid-based theranostic nanomedicines for targeted cancer therapy, Cancers (Basel). 12 (2020) 1–17, https://doi.org/10.3390/cancers12040940.
[32] B. Zhang, P. Wei, Z. Zhou, T. Wei, Interactions of graphene with mammalian cells: Molecular mechanisms and biomedical insights, Adv. Drug Deliv. Rev. 105 (2016) 145–162, https://doi.org/10.1016/j.addr.2016.08.009.
[33] A.M. Pinto, J.A. Moreira, F.D. Magalhães, I.C. Gonçalves, Polymer surface adsorption as a strategy to improve the biocompatibility of graphene nanoplatelets, Colloids Surfaces B Biointerfaces. 146 (2016) 818–824, https://doi.org/10.1016/j.colsurfb.2016.07.031.
[34] M. Xu, J. Zhu, F. Wang, Y. Xiong, Y. Wu, Q. Wang, J. Weng, Z. Zhang, W. Chen, S. Liu, Improved In Vitro and In Vivo Biocompatibility of Graphene Oxide through Surface Modification: Poly(Acrylic Acid)-Functionalization is Superior to PEGylation, ACS Nano. 10 (2016) 3267–3281, https://doi.org/10.1021/acsnano.6b00539.
[35] Z. Liu, J.T. Robinson, X. Sun, H. Dai, PEGylated nanographene oxide for delivery of water-insoluble cancer drugs, J. Am. Chem. Soc. 130 (2008) 10876–10877, https://doi.org/10.1021/ja803688x.
[36] Z. Xu, S. Wang, Y. Li, M. Wang, P. Shi, X. Huang, Covalent functionalization of graphene oxide with biocompatible poly(ethylene glycol) for delivery of paclitaxel, ACS Appl. Mater. Interfaces. 6 (2014) 17268–17276, https://doi.org/10.1021/am505308f.
[37] S.M. Chowdhury, C. Surhland, Z. Sanchez, P. Chaudhary, M.A. Suresh Kumar, S. Lee, L.A. Peña, M. Waring, B. Sitharaman, M. Naidu, Graphene nanoribbons as a drug delivery agent for lucanthone mediated therapy of glioblastoma multiforme, Nanomedicine Nanotechnology, Biol. Med. 11 (2015) 109–118, https://doi.org/10.1016/j.nano.2014.08.001.
[38] J. Chu, P. Shi, W. Yan, J. Fu, Z. Yang, C. He, X. Deng, H. Liu, PEGylated graphene oxide-mediated quercetin-modified collagen hybrid scaffold for enhancement of MSCs differentiation potential and diabetic wound healing, Nanoscale. 10 (2018) 9547–9560, https://doi.org/10.1039/c8nr02538j.
[39] K. Yang, Ḱ.J. Wan, Ḱ.S. Zhang, Y. Zhang, S. Lee, Z. Liu, PEGylated Graphene in Mice, ACS Nano. 5 (2011) 516–522.
[40] K. Yang, H. Gong, X. Shi, J. Wan, Y. Zhang, Z. Liu, In vivo biodistribution and toxicology of functionalized nano-graphene oxide in mice after oral and intraperitoneal administration, Biomaterials. 34 (2013) 2787–2795, https://doi.org/10.1016/j.biomaterials.2013.01.001.
[41] P. Khramtsov, M. Bochkova, V. Timganova, A. Nechaev, S. Uzhviyuk, K. Shardina, I. Maslennikova, M. Rayev, S. Zamorina, Interaction of Graphene Oxide Modified with Linear and Branched PEG with Monocytes Isolated from Human Blood, Nanomaterials. 12 (2021) 126, https://doi.org/10.3390/nano12010126.
[42] F. Liu, D. Yang, Y. Liu, Q. Cao, Y. Sun, Q. Wang, H. Tang, Improving dispersive property, biocompatibility and targeting gene transfection of graphene oxide by covalent attachment of polyamidoamine dendrimer and glycyrrhetinic acid, Colloids Surfaces B Biointerfaces. 171 (2018) 622–628, https://doi.org/10.1016/j.colsurfb.2018.07.067.
[43] W. Liang, Y.u. Huang, D. Lu, X. Ma, T. Gong, X. Cui, B. Yu, C. Yang, C. Dong, S. Shuang, Β-Cyclodextrin-Hyaluronic Acid Polymer Functionalized Magnetic Graphene Oxide Nanocomposites for Targeted Photo-Chemotherapy of Tumor Cells, Polymers (Basel). 11 (1) (2019) 133.
[44] S. Borandeh, A. Abdolmaleki, S.S. Abolmaali, A.M. Tamaddon, Synthesis, structural and in-vitro characterization of β-cyclodextrin grafted L-phenylalanine functionalized graphene oxide nanocomposite: A versatile nanocarrier for pH-sensitive doxorubicin delivery, Carbohydr. Polym. 201 (2018) 151–161, https://doi.org/10.1016/j.carbpol.2018.08.064.
[45] Y. Yang, Y.M. Zhang, Y. Chen, D. Zhao, J.T. Chen, Y. Liu, Construction of a graphene oxide based noncovalent multiple nanosupramolecular assembly as a scaffold for drug delivery, Chem. - A Eur. J. 18 (2012) 4208–4215, https://doi.org/10.1002/chem.201103445.
[46] J. Tan, N. Meng, Y. Fan, Y. Su, M. Zhang, Y. Xiao, N. Zhou, Hydroxypropyl-β-cyclodextrin-graphene oxide conjugates: Carriers for anti-cancer drugs, Mater. Sci. Eng. C. 61 (2016) 681–687, https://doi.org/10.1016/j.msec.2015.12.098.
[47] M. Pooresmaeil, H. Namazi, Fabrication of a smart and biocompatible brush copolymer decorated on magnetic graphene oxide hybrid nanostructure for drug delivery application, Eur. Polym. J. 142 (2021), https://doi.org/10.1016/j.eurpolymj.2020.110126 110126.
[48] R. Kurapati, F. Bonachera, J. Russier, A.R. Sureshbabu, C. Ménard-Moyon, K. Kostarelos, A. Bianco, Covalent chemical functionalization enhances the biodegradation of graphene oxide, 2D Mater. 5 (1) (2018) 015020.
[49] W. Hu, C. Peng, M. Lv, X. Li, Y. Zhang, N. Chen, C. Fan, Q. Huang, Protein corona-mediated mitigation of cytotoxicity of graphene oxide, ACS Nano. 5 (2011) 3693–3700, https://doi.org/10.1021/nn200021j.
[50] M. Papi, M.C. Lauriola, V. Palmieri, G. Ciasca, G. Maulucci, M. De Spirito, Plasma protein corona reduces the haemolytic activity of graphene oxide nano and micro flakes, RSC Adv. 5 (2015) 81638–81641, https://doi.org/10.1039/c5ra15083c.
[51] G. Duan, S. Kang, X. Tian, J.A. Garate, L. Zhao, C. Ge, R. Zhou, Protein corona mitigates the cytotoxicity of graphene oxide by reducing its physical interaction with cell membrane, Nanoscale. 7 (2015) 15214–15224, https://doi.org/10.1039/C5NR01839K.
[52] J. Jeong, H.-J. Cho, M. Choi, W.S. Lee, B.H. Chung, J.-S. Lee, In vivo toxicity assessment of angiogenesis and the live distribution of nano-graphene oxide and its PEGylated derivatives using the developing zebrafish embryo, Carbon N. Y. 93 (2015) 431–440, https://doi.org/10.1016/j.carbon.2015.05.024.
[53] S. Sivaselvam, A. Mohankumar, G. Thiruppathi, P. Sundararaj, C. Viswanathan, N. Ponpandian, Engineering the surface of graphene oxide with bovine serum albumin for improved biocompatibility in Caenorhabditis elegans, Nanoscale Adv. 2 (2020) 5219–5230, https://doi.org/10.1039/D0NA00574F.
[54] C. Alibert, B. Goud, J.-B. Manneville, Are cancer cells really softer than normal cells?, Biol Cell. 109 (2017) 167–189, https://doi.org/10.1111/boc.201600078.
[55] Y. Kato, S. Ozawa, C. Miyamoto, Y. Maehata, A. Suzuki, T. Maeda, Y. Baba, Acidic extracellular microenvironment and cancer, Cancer Cell Int. 13 (2013) 89, https://doi.org/10.1186/1475-2867-13-89.
[56] N. Bernardes, A. Fialho, Perturbing the Dynamics and Organization of Cell Membrane Components: A New Paradigm for Cancer-Targeted Therapies, Int. J. Mol. Sci. 19 (2018) 3871, https://doi.org/10.3390/ijms19123871.
[57] L.S. Franqui, M.A. De Farias, R.V. Portugal, C.A.R. Costa, R.R. Domingues, A.G. Souza Filho, V.R. Coluci, A.F.P. Leme, D.S.T. Martinez, Interaction of graphene oxide with cell culture medium: Evaluating the fetal bovine serum protein corona formation towards in vitro nanotoxicity assessment and nanobiointeractions, Mater. Sci. Eng. C. 100 (2019) 363–377, https://doi.org/10.1016/j.msec.2019.02.066.
[58] R. Di Santo, L. Digiacomo, E. Quagliarini, A.L. Capriotti, A. Laganà, R.Z. Chiozzi, D. Caputo, C. Cascone, R. Coppola, D. Pozzi, G. Caracciolo, Personalized graphene oxide-protein corona in the human plasma of pancreatic cancer patients, Front. Bioeng, Biotechnol. 8 (2020) 1–11, https://doi.org/10.3389/fbioe.2020.00491.
[59] N.S. Ekal, R. Patil, N. Ranjan, P. Bahadur, S. Tiwari, Oxidation state of graphene oxide nanosheets drives their interaction with proteins: A case of bovine serum albumin, Colloids Surfaces B Biointerfaces. 212 (2022), https://doi.org/10.1016/j.colsurfb.2022.112367 112367.
[60] M. de Sousa, C.H.Z. Martins, L.S. Franqui, L.C. Fonseca, F.S. Delite, E.M. Lanzoni, D.S.T. Martinez, O.L. Alves, Covalent functionalization of graphene oxide with <scp>d</scp> -mannose: evaluating the hemolytic effect and protein corona formation, J. Mater. Chem. B. 6 (2018) 2803–2812, https://doi.org/10.1039/C7TB02997G.
[61] R. Di Santo, L. Digiacomo, E. Quagliarini, A.L. Capriotti, A. Laganà, R. Zenezini Chiozzi, D. Caputo, C. Cascone, R. Coppola, D. Pozzi, G. Caracciolo, Personalized Graphene Oxide-Protein Corona in the Human Plasma of Pancreatic Cancer Patients, Front. Bioeng. Biotechnol. 8 (2020), https://doi.org/10.3389/fbioe.2020.00491.
[62] N. Chatterjee, H.J. Eom, J. Choi, A systems toxicology approach to the surface functionality control of graphene-cell interactions, Biomaterials. 35 (2014) 1109–1127, https://doi.org/10.1016/j.biomaterials.2013.09.108.
[63] M. Farahani, M. Rezaei-Tavirani, H. Zali, A. Arefi Oskouie, M. Omidi, A. Lashay, Deciphering the transcription factor-microRNA-target gene regulatory network associated with graphene oxide cytotoxicity, Nanotoxicology. 12 (2018) 1014–1026, https://doi.org/10.1080/17435390.2018.1513090.
[64] Y. Liao, W. Wang, Z. Li, Y. Wang, L. Zhang, X. Huang, P. Cai, Comparative proteomic analysis reveals cytotoxicity induced by graphene oxide exposure in A549 cells, J. Appl. Toxicol. 41 (2021) 1103–1114, https://doi.org/10.1002/jat.4096.
[65] J. Linares, M.C. Matesanz, M. Vila, M.J. Feito, G. Gonçalves, M. Vallet-Regí, P.A. A.P. Marques, M.T. Portolés, Endocytic mechanisms of graphene oxide nanosheets in osteoblasts, hepatocytes and macrophages, ACS Appl. Mater. Interfaces. 6 (2014) 13697–13706, https://doi.org/10.1021/am5031598.
[66] Q. Mu, G. Su, L. Li, B.O. Gilbertson, L.H. Yu, Q. Zhang, Y.-P. Sun, B. Yan, Size-Dependent Cell Uptake of Protein-Coated Graphene Oxide Nanosheets, ACS Appl. Mater. Interfaces. 4 (2012) 2259–2266, https://doi.org/10.1021/am300253c.
[67] S. Mullick Chowdhury, G. Lalwani, K. Zhang, J.Y. Yang, K. Neville, B. Sitharaman, Cell specific cytotoxicity and uptake of graphene nanoribbons, Biomaterials. 34 (2013) 283–293, https://doi.org/10.1016/j.biomaterials.2012.09.057.
[68] G. Duan, Y. Zhang, B. Luan, J.K. Weber, R.W. Zhou, Z. Yang, L. Zhao, J. Xu, J. Luo, R. Zhou, Graphene-Induced Pore Formation on Cell Membranes, Sci. Rep. 7 (2017) 1–12, https://doi.org/10.1038/srep42767.
[69] T. Lammel, P. Boisseaux, M.L. Fernández-Cruz, J.M. Navas, Internalization and cytotoxicity of graphene oxide and carboxyl graphene nanoplatelets in the

human hepatocellular carcinoma cell line Hep G2, Part. Fibre Toxicol. 10 (2013) 1–21, https://doi.org/10.1186/1743-8977-10-27.
[70] R.G. Mendes, A. Mandarino, B. Koch, A.K. Meyer, A. Bachmatiuk, C. Hirsch, T. Gemming, O.G. Schmidt, Z. Liu, M.H. Rümmeli, Size and time dependent internalization of label-free nano-graphene oxide in human macrophages, Nano Res. 10 (2017) 1980–1995, https://doi.org/10.1007/s12274-016-1385-2.
[71] J. Li, X. Wang, K.-C. Mei, C.H. Chang, J. Jiang, X. Liu, Q. Liu, L.M. Guiney, M.C. Hersam, Y.-P. Liao, H. Meng, T. Xia, Lateral size of graphene oxide determines differential cellular uptake and cell death pathways in Kupffer cells, LSECs, and hepatocytes, Nano Today. 37 (2021), https://doi.org/10.1016/j.nantod.2020.101061 101061.
[72] S.P. Mukherjee, B. Lazzaretto, K. Hultenby, L. Newman, A.F. Rodrigues, N. Lozano, K. Kostarelos, P. Malmberg, B. Fadeel, Graphene Oxide Elicits Membrane Lipid Changes and Neutrophil Extracellular Trap Formation, Chem. 4 (2018) 334–358, https://doi.org/10.1016/j.chempr.2017.12.017.
[73] J. Mao, R. Guo, L.T. Yan, Simulation and analysis of cellular internalization pathways and membrane perturbation for graphene nanosheets, Biomaterials. 35 (2014) 6069–6077, https://doi.org/10.1016/j.biomaterials.2014.03.087.
[74] J. Ma, R. Liu, X. Wang, Q. Liu, Y. Chen, R.P. Valle, Y.Y. Zuo, T. Xia, S. Liu, Crucial Role of Lateral Size for Graphene Oxide in Activating Macrophages and Stimulating Pro-inflammatory Responses in Cells and Animals, ACS Nano. 9 (2015) 10498–10515, https://doi.org/10.1021/acsnano.5b04751.
[75] P.P. Jia, T. Sun, M. Junaid, L. Yang, Y.B. Ma, Z.S. Cui, D.P. Wei, H.F. Shi, D.S. Pei, Nanotoxicity of different sizes of graphene (G) and graphene oxide (GO) in vitro and in vivo, Environ. Pollut. 247 (2019) 595–606, https://doi.org/10.1016/j.envpol.2019.01.072.
[76] K.H. Liao, Y.S. Lin, C.W. MacOsko, C.L. Haynes, Cytotoxicity of graphene oxide and graphene in human erythrocytes and skin fibroblasts, ACS Appl. Mater. Interfaces. 3 (2011) 2607–2615, https://doi.org/10.1021/am200428v.
[77] A.M. Pinto, C. Gonçalves, D.M. Sousa, A.R. Ferreira, J.A. Moreira, I.C. Gonçalves, F.D. Magalhães, Smaller particle size and higher oxidation improves biocompatibility of graphene-based materials, Carbon N. Y. 99 (2016) 318–329, https://doi.org/10.1016/j.carbon.2015.11.076.
[78] M.H. Lim, I.C. Jeung, J. Jeong, S.J. Yoon, S.H. Lee, J. Park, Y.S. Kang, H. Lee, Y.J. Park, H.G. Lee, S.J. Lee, B.S. Han, N.W. Song, S.C. Lee, J.S. Kim, K.H. Bae, J.K. Min, Graphene oxide induces apoptotic cell death in endothelial cells by activating autophagy via calcium-dependent phosphorylation of c-Jun N-terminal kinases, Acta Biomater. 46 (2016) 191–203, https://doi.org/10.1016/j.actbio.2016.09.018.
[79] X. Zhang, J. Yin, C. Peng, W. Hu, Z. Zhu, W. Li, C. Fan, Q. Huang, Distribution and biocompatibility studies of graphene oxide in mice after intravenous administration, Carbon N. Y. 49 (2011) 986–995, https://doi.org/10.1016/j.carbon.2010.11.005.
[80] C. Cheng, S. Nie, S. Li, H. Peng, H. Yang, L. Ma, S. Sun, C. Zhao, Biopolymer functionalized reduced graphene oxide with enhanced biocompatibility via mussel inspired coatings/anchors, J. Mater. Chem. B. 1 (2013) 265–275, https://doi.org/10.1039/c2tb00025c.
[81] G. Qu, X. Wang, Q. Liu, R. Liu, N. Yin, J. Ma, L. Chen, J. He, S. Liu, G. Jiang, The ex vivo and in vivo biological performances of graphene oxide and the impact of surfactant on graphene oxide's biocompatibility, J. Environ. Sci. (China) 25 (2013) 873–881, https://doi.org/10.1016/S1001-0742(12)60252-6.
[82] Z. Chen, C. Yu, I.A. Khan, Y. Tang, S. Liu, M. Yang, Toxic effects of different-sized graphene oxide particles on zebrafish embryonic development, Ecotoxicol. Environ. Saf. 197 (2020), https://doi.org/10.1016/j.ecoenv.2020.110608 110608.
[83] J. Li, X. Zhang, J. Jiang, Y. Wang, H. Jiang, J. Zhang, X. Nie, B. Liu, Systematic Assessment of the Toxicity and Potential Mechanism of Graphene Derivatives In Vitro and In Vivo, Toxicol. Sci. 167 (2019) 269–281, https://doi.org/10.1093/toxsci/kfy235.
[84] J. Chen, G. Zhou, L. Chen, Y. Wang, X. Wang, S. Zeng, Interaction of Graphene and its Oxide with Lipid Membrane: A Molecular Dynamics Simulation Study, J. Phys. Chem. C. 120 (2016) 6225–6231, https://doi.org/10.1021/acs.jpcc.5b10635.
[85] Y. Chen, S. Pandit, S. Rahimi, I. Mijakovic, Interactions Between Graphene-Based Materials and Biological Surfaces: A Review of Underlying Molecular Mechanisms, Adv. Mater. Interfaces. 8 (24) (2021) 2101132.
[86] Y. Tu, M. Lv, P. Xiu, T. Huynh, M. Zhang, M. Castelli, Z. Liu, Q. Huang, C. Fan, H. Fang, R. Zhou, Destructive extraction of phospholipids from Escherichia coli membranes by graphene nanosheets, Nat. Nanotechnol. 8 (2013) 594–601, https://doi.org/10.1038/nnano.2013.125.
[87] X. Zhang, F. Cao, L. Wu, X. Jiang, Understanding the Synergic Mechanism of Weak Interactions between Graphene Oxide and Lipid Membrane Leading to the Extraction of Lipids, Langmuir. 35 (2019) 14098–14107, https://doi.org/10.1021/acs.langmuir.9b02536.
[88] L. Zhang, B. Xu, X. Wang, Cholesterol Extraction from Cell Membrane by Graphene Nanosheets: A Computational Study, J. Phys. Chem. B. 120 (2016) 957–964, https://doi.org/10.1021/acs.jpcb.5b10330.
[89] K.E. Kitko, T. Hong, R.M. Lazarenko, D. Ying, Y.-Q. Xu, Q. Zhang, Membrane cholesterol mediates the cellular effects of monolayer graphene substrates, Nat. Commun. 9 (2018) 796, https://doi.org/10.1038/s41467-018-03185-0.
[90] Z. Tu, K. Achazi, A. Schulz, R. Mülhaupt, S. Thierbach, E. Rühl, M. Adeli, R. Haag, Combination of Surface Charge and Size Controls the Cellular Uptake of Functionalized Graphene Sheets, Adv. Funct. Mater. 27 (2017) 1701837, https://doi.org/10.1002/adfm.201701837.
[91] W. Majeed, S. Bourdo, D.M. Petibone, V. Saini, K.B. Vang, Z.A. Nima, K.M. Alghazali, E. Darrigues, A. Ghosh, F. Watanabe, D. Casciano, S.F. Ali, A.S. Biris, The role of surface chemistry in the cytotoxicity profile of graphene, J. Appl. Toxicol. 37 (2017) 462–470, https://doi.org/10.1002/jat.3379.
[92] F.F. Contreras-Torres, A. Rodríguez-Galván, C.E. Guerrero-Beltrán, E. Martínez-Lorán, E. Vázquez-Garza, N. Ornelas-Soto, G. García-Rivas, Differential cytotoxicity and internalization of graphene family nanomaterials in myocardial cells, Mater. Sci. Eng. C. 73 (2017) 633–642, https://doi.org/10.1016/j.msec.2016.12.080.
[93] R. Li, L.M. Guiney, C.H. Chang, N.D. Mansukhani, Z. Ji, X. Wang, Y.P. Liao, W. Jiang, B. Sun, M.C. Hersam, A.E. Nel, T. Xia, Surface Oxidation of Graphene Oxide Determines Membrane Damage, Lipid Peroxidation, and Cytotoxicity in Macrophages in a Pulmonary Toxicity Model, ACS Nano. 12 (2018) 1390–1402, https://doi.org/10.1021/acsnano.7b07737.
[94] N. Chatterjee, J.S. Yang, K. Park, S.M. Oh, J. Park, J. Choi, Screening of toxic potential of graphene family nanomaterials using in vitro and alternative in vivo toxicity testing systems, Environ. Health Toxicol. 30 (2015) e2015007.
[95] B.F.M. Ribeiro, M.M. Souza, D.S. Fernandes, D.R. Carmo, G.M. Machado-Santelli, Graphene oxide-based nanomaterial interaction with human breast cancer cells, J. Biomed. Mater. Res. - Part A. 108 (4) (2020) 863–870.
[96] Y. Li, Q. Wu, Y. Zhao, Y. Bai, P. Chen, T. Xia, D. Wang, Response of MicroRNAs to in vitro treatment with graphene oxide, ACS Nano. 8 (2014) 2100–2110, https://doi.org/10.1021/nn4065378.
[97] J. Wu, R. Yang, L. Zhang, Z. Fan, S. Liu, Cytotoxicity effect of graphene oxide on human MDA-MB-231 cells, Toxicol. Mech. Methods. 25 (2015) 312–319, https://doi.org/10.3109/15376516.2015.1031415.
[98] T. Chen, Q. Zhang, Y. Song, A.N. Isak, X. Tang, H. Wang, Z. Ma, F. Sun, Q. Pan, X. Zhu, Spatial confinement of chemically engineered cancer cells using large graphene oxide sheets: a new mode of cancer therapy, Nanoscale Horizons. 6 (2021) 979–986, https://doi.org/10.1039/D1NH00350J.
[99] M.C. Matesanz, M. Vila, M.J. Feito, J. Linares, G. Gonçalves, M. Vallet-Regi, P.A. A.P. Marques, M.T. Portolés, The effects of graphene oxide nanosheets localized on F-actin filaments on cell-cycle alterations, Biomaterials. 34 (2013) 1562–1569, https://doi.org/10.1016/j.biomaterials.2012.11.001.
[100] S. Bera, S. Ghosh, A. Ali, M. Pal, P. Chakrabarti, Inhibition of microtubule assembly and cytotoxic effect of graphene oxide on human colorectal carcinoma cell HCT116, Arch. Biochem. Biophys. 708 (2021), https://doi.org/10.1016/j.abb.2021.108940 108940.
[101] B.F.M. Ribeiro, M.M. Souza, D.S. Fernandes, D.R. Carmo, G.M. Machado-Santelli, Graphene oxide-based nanomaterial interaction with human breast cancer cells, J. Biomed. Mater. Res. Part A. 108 (2020) 863–870, https://doi.org/10.1002/jbm.a.36864.
[102] J. Zhu, M. Xu, M. Gao, Z. Zhang, Y. Xu, T. Xia, S. Liu, Graphene Oxide Induced Perturbation to Plasma Membrane and Cytoskeletal Meshwork Sensitize Cancer Cells to Chemotherapeutic Agents, ACS Nano. 11 (2017) 2637–2651, https://doi.org/10.1021/acsnano.6b07311.
[103] X. Ji, B. Xu, M. Yao, Z. Mao, Y. Zhang, G. Xu, Q. Tang, X. Wang, Y. Xia, Graphene oxide quantum dots disrupt autophagic flux by inhibiting lysosome activity in GC-2 and TM4 cell lines, Toxicology. 374 (2016) 10–17, https://doi.org/10.1016/j.tox.2016.11.009.
[104] X. Feng, L. Chen, W. Guo, Y. Zhang, X. Lai, L. Shao, Y. Li, Graphene oxide induces p62/SQSTM-dependent apoptosis through the impairment of autophagic flux and lysosomal dysfunction in PC12 cells, Acta Biomater. 81 (2018) 278–292, https://doi.org/10.1016/j.actbio.2018.09.057.
[105] L. Liu, M. Zhang, Q. Zhang, W. Jiang, Graphene nanosheets damage the lysosomal and mitochondrial membranes and induce the apoptosis of RBL-2H3 cells, Sci. Total Environ. 734 (2020), https://doi.org/10.1016/j.scitotenv.2020.139229 139229.
[106] D.Y. Zhang, Y. Zheng, C.P. Tan, J.H. Sun, W. Zhang, L.N. Ji, Z.W. Mao, Graphene Oxide Decorated with Ru(II)-Polyethylene Glycol Complex for Lysosome-Targeted Imaging and Photodynamic/Photothermal Therapy, ACS Appl. Mater. Interfaces. 9 (2017) 6761–6771, https://doi.org/10.1021/acsami.6b13808.
[107] Y. Li, Y. Liu, Y. Fu, T. Wei, L. Le Guyader, G. Gao, R.S. Liu, Y.Z. Chang, C. Chen, The triggering of apoptosis in macrophages by pristine graphene through the MAPK and TGF-beta signaling pathways, Biomaterials. 33 (2012) 402–411, https://doi.org/10.1016/j.biomaterials.2011.09.091.
[108] W. Zhang, L. Yan, M. Li, R. Zhao, X. Yang, T. Ji, Z. Gu, J.J. Yin, X. Gao, G. Nie, Deciphering the underlying mechanisms of oxidation-state dependent cytotoxicity of graphene oxide on mammalian cells, Toxicol. Lett. 237 (2015) 61–71, https://doi.org/10.1016/j.toxlet.2015.05.021.
[109] S. Jaworski, B. Strojny, E. Sawosz, M. Wierzbicki, M. Grodzik, M. Kutwin, K. Daniluk, A. Chwalibog, Degradation of Mitochondria and Oxidative Stress as the Main Mechanism of Toxicity of Pristine Graphene on U87 Glioblastoma Cells and Tumors and HS-5 Cells, Int. J. Mol. Sci. 20 (2019) 650, https://doi.org/10.3390/ijms20030650.
[110] J. Zhang, L. Yan, P. Wei, R. Zhou, C. Hua, M. Xiao, Y. Tu, Z. Gu, T. Wei, PEG-GO@XN nanocomposite suppresses breast cancer metastasis via inhibition of mitochondrial oxidative phosphorylation and blockade of epithelial-to-mesenchymal transition, Eur. J. Pharmacol. 895 (2021), https://doi.org/10.1016/j.ejphar.2021.173866 173866.
[111] I.I.J. Alsaedi, Z.J. Taqi, A.M. Abdul Hussien, G.M. Sulaiman, M.S. Jabir, Graphene nanoparticles induces apoptosis in MCF-7 cells through mitochondrial damage and NF-KB pathway, Mater. Res. Express. 6 (9) (2019) 095413.

[112] Y. Qin, Z.W. Zhou, S.T. Pan, Z.X. He, X. Zhang, J.X. Qiu, W. Duan, T. Yang, S.F. Zhou, Graphene quantum dots induce apoptosis, autophagy, and inflammatory response via p38 mitogen-activated protein kinase and nuclear factor-κB mediated signaling pathways in activated THP-1 macrophages, Toxicology. 327 (2015) 62–76, https://doi.org/10.1016/j.tox.2014.10.011.
[113] P. Kalluru, R. Vankayala, C.S. Chiang, K.C. Hwang, Nano-graphene oxide-mediated In vivo fluorescence imaging and bimodal photodynamic and photothermal destruction of tumors, Biomaterials. 95 (2016) 1–10, https://doi.org/10.1016/j.biomaterials.2016.04.006.
[114] L. Wang, D. Yu, R. Dai, D. Fu, W. Li, Z. Guo, C. Cui, J. Xu, S. Shen, K. Ma, PEGylated doxorubicin cloaked nano-graphene oxide for dual-responsive photochemical therapy, Int. J. Pharm. 557 (2019) 66–73, https://doi.org/10.1016/j.ijpharm.2018.12.037.
[115] F. Shaheen, M. Aziz, M. Fatima, M. Khan, F. Ahmed, R. Ahmad, M. Ahmad, T. Alkhuraiji, M. Akram, R. Raza, S. Ali, In vitro cytotoxicity and morphological assessments of GO-ZnO against the MCF-7 cells: Determination of singlet oxygen by chemical trapping, Nanomaterials. 8 (7) (2018) 539.
[116] T.A. Tabish, S. Zhang, P.G. Winyard, Developing the next generation of graphene-based platforms for cancer therapeutics: The potential role of reactive oxygen species, Redox Biol. 15 (2018) 34–40, https://doi.org/10.1016/j.redox.2017.11.018.
[117] C. Zhang, Z. Liu, Y. Zheng, Y. Geng, C. Han, Y. Shi, H. Sun, C. Zhang, Y. Chen, L. Zhang, Q. Guo, L. Yang, X. Zhou, L. Kong, Glycyrrhetinic Acid Functionalized Graphene Oxide for Mitochondria Targeting and Cancer Treatment In Vivo, Small. 14 (2018) 1703306, https://doi.org/10.1002/smll.201703306.
[118] C. Jin, F. Wang, Y. Tang, X. Zhang, J. Wang, Y. Yang, Distribution of graphene oxide and TiO2-graphene oxide composite in A549 cells, Biol. Trace Elem. Res. 159 (2014) 393–398, https://doi.org/10.1007/s12011-014-0027-3.
[119] A. Zuchowska, E. Jastrzebska, M. Mazurkiewicz-Pawlicka, A. Malolepszy, L. Stobinski, M. Trzaskowski, Z. Brzozka, Well-defined Graphene Oxide as a Potential Component in Lung Cancer Therapy, Curr. Cancer Drug Targets. 20 (2020) 47–58, https://doi.org/10.2174/1568009619666191021113807.
[120] L. Qi, T. Pan, L. Ou, Z. Ye, C. Yu, B. Bao, Z. Wu, D. Cao, L. Dai, Biocompatible nucleus-targeted graphene quantum dots for selective killing of cancer cells via DNA damage, Commun. Biol. 4 (2021) 214, https://doi.org/10.1038/s42003-021-01713-1.
[121] C. Wang, C. Wu, X. Zhou, T. Han, X. Xin, J. Wu, J. Zhang, S. Guo, Enhancing Cell Nucleus Accumulation and DNA Cleavage Activity of Anti-Cancer Drug via Graphene Quantum Dots, Sci. Rep. 3 (2013) 1–8, https://doi.org/10.1038/srep02852.
[122] K.-C. Lin, M.-W. Lin, M.-N. Hsu, G. Yu-Chen, Y.-C. Chao, H.-Y. Tuan, C.-S. Chiang, Y.-C. Hu, Graphene oxide sensitizes cancer cells to chemotherapeutics by inducing early autophagy events, promoting nuclear trafficking and necrosis, Theranostics. 8 (2018) 2477–2487, https://doi.org/10.7150/thno.24173.
[123] G.Y. Chen, C. Le Meng, K.C. Lin, H.Y. Tuan, H.J. Yang, C.L. Chen, K.C. Li, C.S. Chiang, Y.C. Hu, Graphene oxide as a chemosensitizer: Diverted autophagic flux, enhanced nuclear import, elevated necrosis and improved antitumor effects, Biomaterials. 40 (2015) 12–22, https://doi.org/10.1016/j.biomaterials.2014.11.034.
[124] L. Di Cristo, S. Mc Carthy, K. Paton, D. Movia, A. Prina-Mello, Interplay between oxidative stress and endoplasmic reticulum stress mediated-autophagy in unfunctionalised few-layer graphene-exposed macrophages, 2D Mater. 5 (2018), https://doi.org/10.1088/2053-1583/aadf45 045033.
[125] R.D. Wagner, S.J. Johnson, Z.Y. Danielsen, J.-H. Lim, T. Mudalige, S. Linder, Polyethylene glycol-functionalized poly (Lactic Acid-co-Glycolic Acid) and graphene oxide nanoparticles induce pro-inflammatory and apoptotic responses in Candida albicans-infected vaginal epithelial cells, PLoS One. 12 (2017) e0175250. https://doi.org/10.1371/journal.pone.0175250.
[126] A. Chwalibog, S. Jaworski, E. Sawosz, M. Kutwin, M. Wierzbicki, M. Hinzmann, M. Grodzik, A. Winnicka, L. Lipinska, K. Wlodyga, In vitro and in vivo effects of graphene oxide and reduced graphene oxide on glioblastoma, Int. J. Nanomedicine. (2015) 1585, https://doi.org/10.2147/IJN.S77591.
[127] S. Pandey, A. Nandi, S. Basu, N. Ballav, Inducing endoplasmic reticulum stress in cancer cells using graphene oxide-based nanoparticles, Nanoscale Adv. 2 (2020) 4887–4894, https://doi.org/10.1039/D0NA00338G.
[128] Y. Luo, J. Peng, C. Huang, Y. Cao, Graphene oxide size-dependently altered lipid profiles in THP-1 macrophages, Ecotoxicol. Environ. Saf. 199 (2020), https://doi.org/10.1016/j.ecoenv.2020.110714 110714.
[129] T.C. Walther, R.V. Farese, Lipid Droplets and Cellular Lipid Metabolism, Annu. Rev. Biochem. 81 (1) (2012) 687–714.
[130] L.M. Saeed, M. Mahmood, S.J. Pyrek, T. Fahmi, Y. Xu, T. Mustafa, Z.A. Nima, S. M. Bratton, D. Casciano, E. Dervishi, A. Radominska-Pandya, A.S. Biris, Single-walled carbon nanotube and graphene nanodelivery of gambogic acid increases its cytotoxicity in breast and pancreatic cancer cells, J. Appl. Toxicol. 34 (2014) 1188–1199, https://doi.org/10.1002/jat.3018.
[131] K. Wang, K. Wang, J. Ruan, H. Song, J. Zhang, Y. Wo, S. Guo, D. Cui, Biocompatibility of Graphene Oxide Biocompatibility of Graphene Oxide, Nanoscale Res Lett. 6 (2010) 8. http://www.nanoscalereslett.com/content/6/1/8.
[132] C. Sun, D.L. Wakefield, Y. Han, D.A. Muller, D.A. Holowka, B.A. Baird, W.R. Dichtel, Graphene Oxide Nanosheets Stimulate Ruffling and Shedding of Mammalian Cell Plasma Membranes, Chem. 1 (2016) 273–286, https://doi.org/10.1016/j.chempr.2016.06.019.
[133] M. Pumera, Graphene Oxide Stimulates Cells to Ruffle and Shed Plasma Membranes, Chem. 1 (2016) 189–190, https://doi.org/10.1016/j.chempr.2016.07.008.
[134] Y. Tang, H. Hu, M.G. Zhang, J. Song, L. Nie, S. Wang, G. Niu, P. Huang, G. Lu, X. Chen, An aptamer-targeting photoresponsive drug delivery system using "off–on" graphene oxide wrapped mesoporous silica nanoparticles, Nanoscale. 7 (2015) 6304–6310, https://doi.org/10.1039/C4NR07493A.
[135] M. Sosnowska, M. Kutwin, B. Strojny, P. Koczoń, J. Szczepaniak, J. Bałaban, K. Daniluk, S. Jaworski, A. Chwalibog, W. Bielawski, E. Sawosz, Graphene oxide nanofilm and chicken embryo extract decrease the invasiveness of HepG2 liver cancer cells, Cancer Nanotechnol. 12 (2021) 2, https://doi.org/10.1186/s12645-020-00073-5.
[136] K. Vinothini, N.K. Rajendran, A. Ramu, N. Elumalai, M. Rajan, Folate receptor targeted delivery of paclitaxel to breast cancer cells via folic acid conjugated graphene oxide grafted methyl acrylate nanocarrier, Biomed. Pharmacother. 110 (2019) 906–917, https://doi.org/10.1016/j.biopha.2018.12.008.
[137] X. Cui, L. Dong, S. Zhong, C. Shi, Y. Sun, P. Chen, Sonochemical fabrication of folic acid functionalized multistimuli-responsive magnetic graphene oxide-based nanocapsules for targeted drug delivery, Chem. Eng. J. 326 (2017) 839–848, https://doi.org/10.1016/j.cej.2017.06.045.
[138] C. Martín, A. Ruiz, S. Keshavan, G. Reina, D. Murera, Y. Nishina, B. Fadeel, A. Bianco, A Biodegradable Multifunctional Graphene Oxide Platform for Targeted Cancer Therapy, Adv. Funct. Mater. 29 (2019) 1901761, https://doi.org/10.1002/adfm.201901761.
[139] E. Masoudipour, S. Kashanian, N. Maleki, A targeted drug delivery system based on dopamine functionalized nano graphene oxide, Chem. Phys. Lett. 668 (2017) 56–63, https://doi.org/10.1016/j.cplett.2016.12.019.
[140] T. Jiang, W. Sun, Q. Zhu, N.A. Burns, S.A. Khan, R. Mo, Z. Gu, Furin-mediated sequential delivery of anticancer cytokine and small-molecule drug shuttled by graphene, Adv. Mater. 27 (2015) 1021–1028, https://doi.org/10.1002/adma.201404498.
[141] Y. Zeng, Z. Yang, H. Li, Y. Hao, C. Liu, L. Zhu, J. Liu, B. Lu, R. Li, Multifunctional Nanographene Oxide for Targeted Gene-Mediated Thermochemotherapy of Drug-resistant Tumour, Sci. Rep. 7 (2017) 1–10, https://doi.org/10.1038/srep43506.
[142] T. Lu, Z. Nong, L. Wei, M. Wei, G. Li, N. Wu, C. Liu, B. Tang, Q. Qin, X. Li, F. Meng, Preparation and anti-cancer activity of transferrin/folic acid double-targeted graphene oxide drug delivery system, J. Biomater. Appl. 35 (2020) 15–27, https://doi.org/10.1177/0885328220913976.
[143] Y. Fong, C.-H. Chen, J.-P. Chen, Intratumoral Delivery of Doxorubicin on Folate-Conjugated Graphene Oxide by In-Situ Forming Thermo-Sensitive Hydrogel for Breast Cancer Therapy, Nanomaterials. 7 (2017) 388, https://doi.org/10.3390/nano7110388.
[144] J. Li, X. Huang, R. Huang, J. Jiang, Y. Wang, J. Zhang, H. Jiang, X. Xiang, W. Chen, X. Nie, R. Gui, Erythrocyte membrane camouflaged graphene oxide for tumor-targeted photothermal-chemotherapy, Carbon N. Y. 146 (2019) 660–670, https://doi.org/10.1016/j.carbon.2019.02.056.
[145] N. Mauro, C. Scialabba, S. Agnello, G. Cavallaro, G. Giammona, Folic acid-functionalized graphene oxide nanosheets via plasma etching as a platform to combine NIR anticancer phototherapy and targeted drug delivery, Mater. Sci. Eng. C. 107 (2020), https://doi.org/10.1016/j.msec.2019.110201 110201.
[146] N. Ma, J. Liu, W. He, Z. Li, Y. Luan, Y. Song, S. Garg, Folic acid-grafted bovine serum albumin decorated graphene oxide: An efficient drug carrier for targeted cancer therapy, J. Colloid Interface Sci. 490 (2017) 598–607, https://doi.org/10.1016/j.jcis.2016.11.097.
[147] Y. Guo, H. Xu, Y. Li, F. Wu, Y. Li, Y. Bao, X. Yan, Z. Huang, P. Xu, Hyaluronic acid and Arg-Gly-Asp peptide modified Graphene oxide with dual receptor-targeting function for cancer therapy, J. Biomater. Appl. 32 (2017) 54–65, https://doi.org/10.1177/0885328217712110.
[148] B.S. Dash, Y.-J. Lu, H.-A. Chen, C.-C. Chuang, J.-P. Chen, Magnetic and GRPR-targeted reduced graphene oxide/doxorubicin nanocomposite for dual-targeted chemo-photothermal cancer therapy, Mater. Sci. Eng. C. 128 (2021), https://doi.org/10.1016/j.msec.2021.112311 112311.
[149] A. Halim, Q. Luo, Y. Ju, G. Song, A mini review focused on the recent applications of graphene oxide in stem cell growth and differentiation, Nanomaterials. 8 (9) (2018) 736.
[150] M. Fiorillo, A.F. Verre, M. Iliut, M. Peiris-Pagés, B. Ozsvari, R. Gandara, A.R. Cappello, F. Sotgia, A. Vijayaraghavan, M.P. Lisanti, Graphene oxide selectively targets cancer stem cells, across multiple tumor types: Implications for non-toxic cancer treatment, via "differentiation-based nano-therapy, Oncotarget. 6 (2015) 3553–3562, https://doi.org/10.18632/oncotarget.3348.
[151] S. Gurunathan, J.-H. Kim, Graphene Oxide-Silver Nanoparticles Nanocomposite Stimulates Differentiation in Human Neuroblastoma Cancer Cells (SH-SY5Y), Int. J. Mol. Sci. 18 (2017) 2549, https://doi.org/10.3390/ijms18122549.
[152] C. Martelli, A. King, T. Simon, G. Giamas, Graphene-Induced Transdifferentiation of Cancer Stem Cells as a Therapeutic Strategy against Glioblastoma, ACS Biomater. Sci. Eng. 6 (2020) 3258–3269, https://doi.org/10.1021/acsbiomaterials.0c00197.
[153] Z. Tian, J. Li, S. Zhang, Z. Xu, Y. Yang, D. Kong, H. Zhang, X. Ge, J. Zhang, Z. Liu, Lysosome-Targeted Chemotherapeutics: Half-Sandwich Ruthenium(II) Complexes That Are Selectively Toxic to Cancer Cells, Inorg. Chem. 57 (2018) 10498–10502, https://doi.org/10.1021/acs.inorgchem.8b01944.

[154] B. Zhang, X. Yang, Y. Wang, G. Zhai, Heparin modified graphene oxide for pH-sensitive sustained release of doxorubicin hydrochloride, Mater. Sci. Eng. C. 75 (2017) 198–206, https://doi.org/10.1016/j.msec.2017.02.048.

[155] S. Gurunathan, M. Arsalan Iqbal, M. Qasim, C.H. Park, H. Yoo, J.H. Hwang, S.J. Uhm, H. Song, C. Park, J.T. Do, Y. Choi, J.-H. Kim, K. Hong, Evaluation of graphene oxide induced cellular toxicity and transcriptome analysis in human embryonic kidney cells, Nanomaterials. 9 (7) (2019) 969.